SUPPORTING INFORMATION

Triple-Decker Sandwich Complexes of Tungsten with Planar and Puckered Middle-Decks

Ranjit Bag,[†] Rini Prakash,[†] Suvam Saha,[†] Thierry Roisnel,[‡] and Sundargopal Ghosh[†]*

[†]Department of Chemistry, Indian Institute of Technology Madras, Chennai 600036, India. Tel: +91 44-22574230; Fax: +91 44-22574202; E-mail: sghosh@iitm.ac.in

[‡]Universite de Rennes, CNRS, Institut des Sciences Chimiques de Rennes, UMR 6226, F-35000 Rennes, France.

Table of contents

II Computational details

III Supplementary Data

I Experimental Details

I.1 Crystallographic details

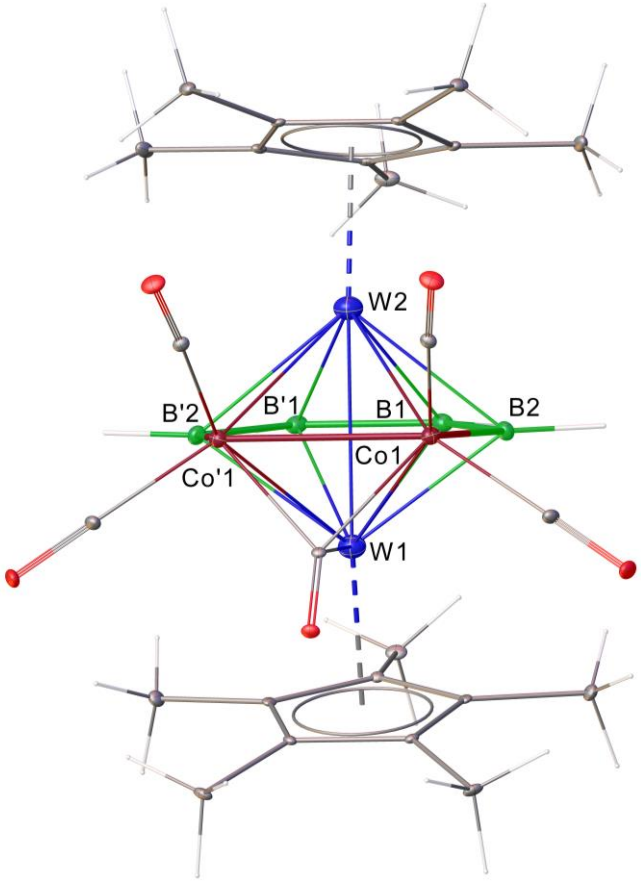

Figure. S1. Molecular structure and labeling diagram of **1**. Bridging hydrogen atoms are not located. Selected bond lengths (Å) and angles (°): W1-W2 2.790, W1-B1 2.221(5), W1-B2 2.257(5), W1-Co1 2.6869(6), W2-B1 2.189(5), W2-B2 2.340(5), W2-Co1 2.7806(7), Co1-Co'1 2.5154(12), Co1-B2 2.125(5), B1-B2 1.708(7), B1-W1-B2 44.84(19), B1-W1-Co1 89.86(13), B2-W1-Co1 49.99(12), Co1-W1-Co'1 55.82(3), B1-W2-B'1 46.5(3), B2-W2-B'2 102.5(2).

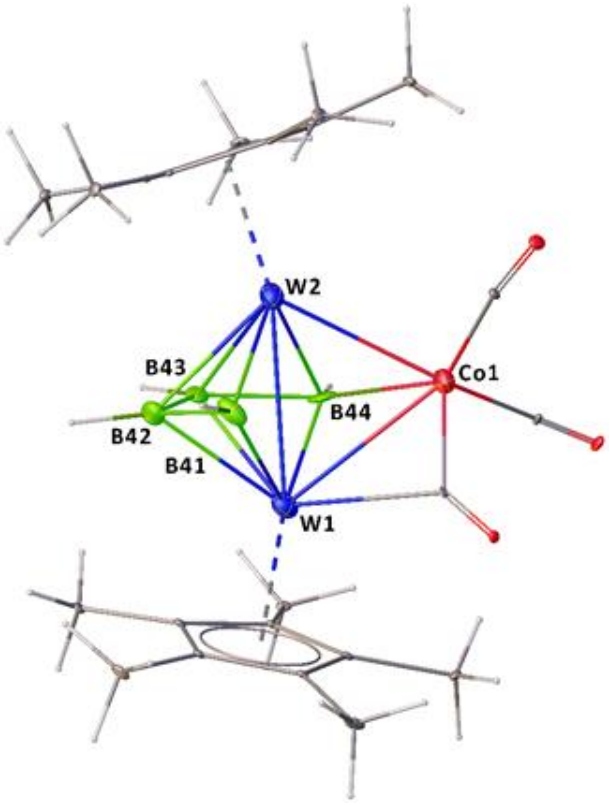

Figure S2. Molecular structure and labeling diagram of **2**. Bridging hydrogen atoms are not located. Selected bond lengths (Å) and angles (°): W1-W2 2.8325(7), W1-Co1 2.7241(17), W2-Co1 2.6185(18), Co1-B44 2.131(15), W1-B44 2.206(14), W1-B41 2.332(15), W2-B41 2.298(14), B41-B42 1.72(2), B42-B43 1.751(19), B43-B44 1.72(2); B44-W1-Co1 49.9(4), Co1-W2-W1 59.81(4), B42-W1-Co1 107.4(3), B44-W1-B43 45.7(5), B44-W1-B42 87.6(5), B43-W2-B41 85.6(5), B44-W1-W2 53.8(4), Co1-W1-W2 56.19(4), B44-B43-B42 123.7(10).

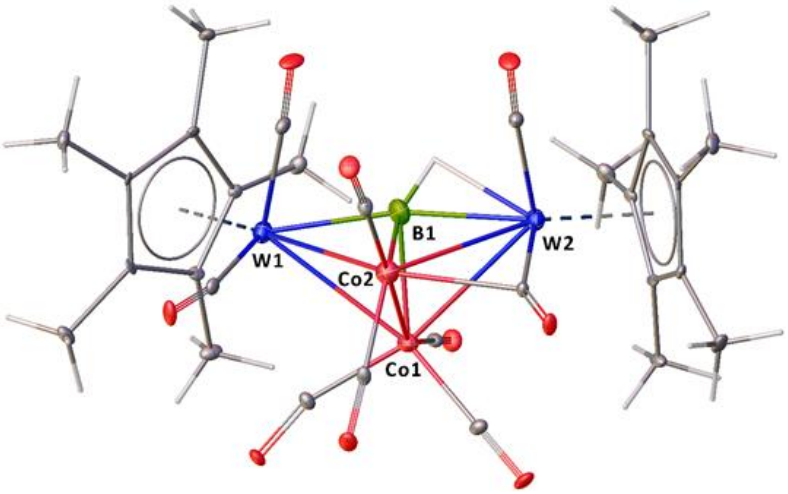

Figure S3. Molecular structure and labelling diagram of **3**. Selected bond lengths (Å) and angles (°): Co1-B1 2.032(14), Co1-W1 2.8029(17), Co1-W2 2.8784(17), Co2-B1 2.083(13), Co2-W1

2.8289(18), Co2-W2 2.6936(18), W1-B1 2.121(13), W2-B1 2.186(13); B1-Co1-Co2 54.3(4), B1-Co1-W1 48.9(4), Co2-Co1-W1 64.69(6), B1-Co1-W2 49.2(4), Co2-Co1-W2 60.03(6), W1-Co1-W2 97.00(5), B1-Co2-Co1 52.4(4), Co1-Co2-W2 67.78(6).

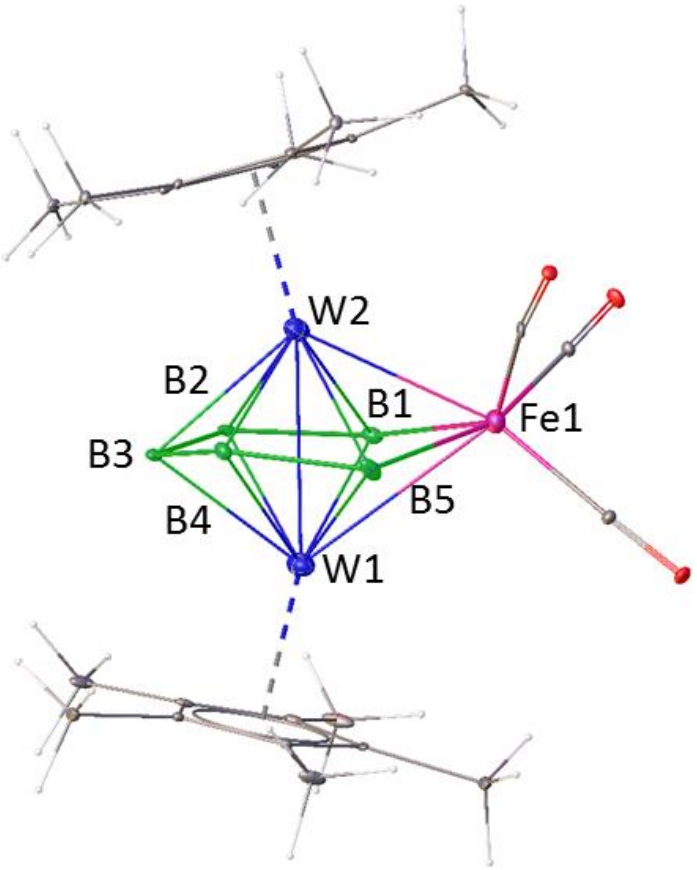

Figure S4. Molecular structure and labeling diagram of **4**. Bridging hydrogens are not located. Selected bond lengths (Å) and angles (°): W1-W2 2.8121(4), W1-Fe1 2.8594(10), B5-Fe1 2.278(10), B1-B2 1.717(13), W2-B5 2.433(10); B1-Fe1-B5 95.3(3), B3-W2-W1 49.2(2), W1-B3-W2 79.0(3), B4-B3-B2 120.7(6), W2-B2-W1 78.5(2).

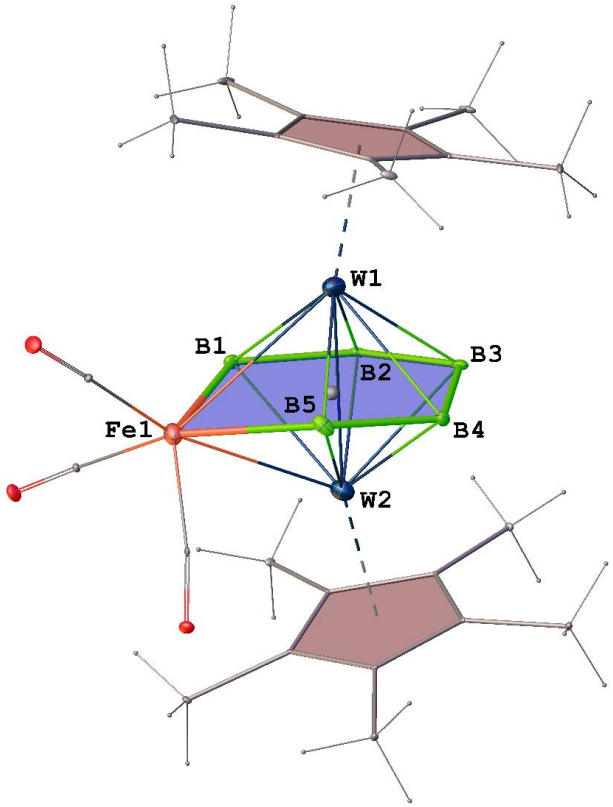

Atom-to-plane distances for B1 Fe1 B5 B4 B3 B2

Label	D/A	Label	D/A	Label	D/A
B1	-0.113	B2	0.052	B3	-0.036
B4	0.124	B5	-0.171	Fe1	0.143

Figure S5. Representation of atomic deviations from the mean plan of [FeB5] in **4**.

I.2 Synthesis and characterization

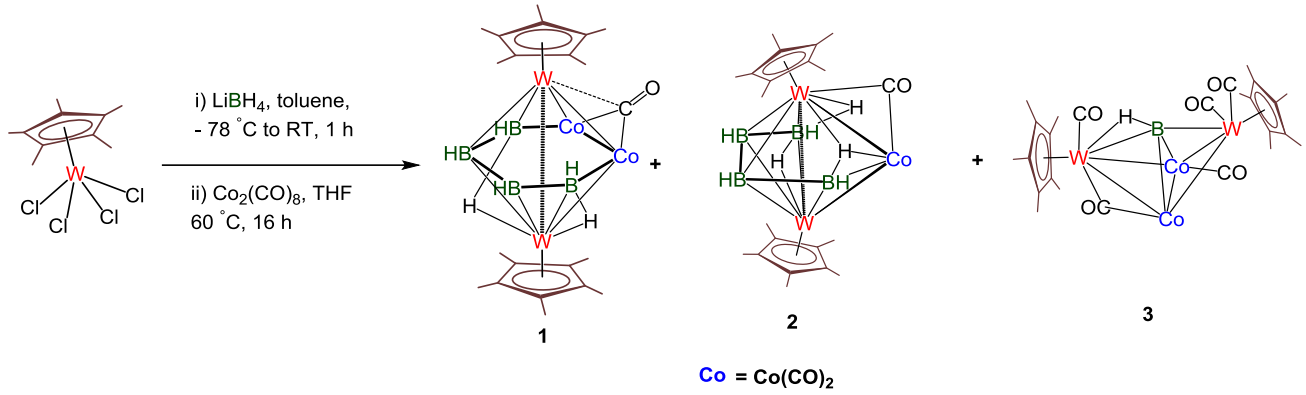

Scheme S1. Synthesis of compound **1, 2,** and **3**

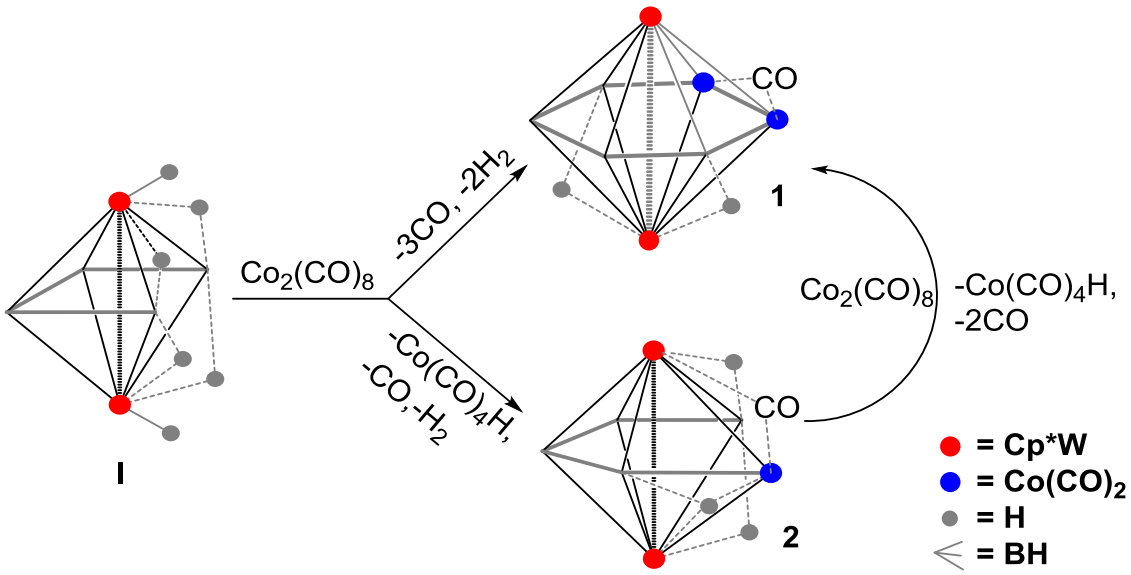

Scheme S2. Possible reaction route for the formation of **1** and **2**.

The calculated positive standard free energy change of the reaction pathways supports the requirement of addition energy for the formation of **1** in both the pathways. Interestingly, complexes **1**, **2** and **I** are related as 6-sep species with *oblatocloso*, *oblatonido* and *oblatoarachno* structures, respectively. Note that, the calculated M-M distance follows the order, **I'>2'>1'** (Cp analogues of **I**, **1** and **2**) which is consistent with their openness.

General Procedures and Instrumentation. All the manipulations were conducted under an atmosphere of dry argon or in vacuo using standard Schlenk line or glove box techniques. Solvents

(hexane, toluene, thf) were purified by distillation from appropriate drying agents-(sodium/benzophenone) under dry argon prior to use. $CDCl_3$ and C_6D_6 were degassed by three freeze-pump-thaw cycles and stored over molecular sieves. Compounds [Cp*WCl_4] was prepared according to literature method,[1] while other chemicals such as, [$LiBH_4$.thf] 2.0 M in THF, Cp*H, n-BuLi, [$Co_2(CO)_8$], and [$Fe_2(CO)_9$] were obtained commercially (Aldrich) and used as received. MeI was purchased from Aldrich and freshly distilled prior to use. The external reference for the ^{11}B NMR, [$Bu_4N(B_3H_8)$] was synthesized with the literature method.[2] Preparative thin layer chromatography was performed with Merck 105554 TLC silica gel 60 F_{254}, layer thickness 250 µm on aluminum sheets (20x20 cm). NMR spectra were recorded on 500 MHz Bruker FT-NMR spectrometers. The residual solvent protons were used as reference (δ, ppm, d_6-benzene, 7.16, $CDCl_3$, 7.26), while a sealed tube containing [$Bu_4N(B_3H_8)$] in d_6-benzene (δ_B, ppm, –30.07) was used as an external reference for the ^{11}B NMR. The infrared spectra were recorded on a JASCO FT/IR-4100 spectrometer in CH_2Cl_2 solvent . Electrospray mass (ESI-MS) spectra were recorded on a Agilent 6545 Q-TOF LC/MS instrument. Due to poor yields and higher sensitivity, satisfactory elemental analysis cannot be obtained for all the compounds. Additionally, the melting point analysis of the compounds shows melting point above 300 °C temperature due to the presence of heavy metals.

Synthesis of 1-3: In a flame-dried Schlenk tube [Cp*WCl_4], (0.1 g, 0.21 mmol) in 10 mL of toluene was treated with 5-fold excess of [$LiBH_4$·THF] (0.7 mL) at -78 °C and allowed to stir at room temperature for 1 h. After removal of toluene, the residue was extracted into hexane and filtered through a frit using Celite. The brownish-green hexane extract was dried in vacuo, and taken in 10 mL of THF and heated at 60 °C in presence of [$Co_2(CO)_8$] (0.03 g) for 16 h. The solvent was evaporated in vacuo followed by the extraction of the residue into hexane and passing it through Celite. After removal of solvent from the filtrate, the residue was subjected to chromatographic workup using silica gel TLC plates. Elution with a hexane/CH_2Cl_2 (70:30 v/v) mixture yielded brown **1** (0.012 g, 12 %), violet **2** (0.010 g, 11 %) and orange **3** (0.016 g, 14 %) along with the known [$(Cp^*W)_2B_5H_9$][3] (0.018 g, 23 %).

1: MS (ESI+): *m/z* calculated for $[M-(3H+3Co)]^+$ 859.0570, found 859.1361; $^{11}B\{^1H\}$ NMR (160 MHz, $CDCl_3$, 22 °C): δ = 91.8 (s, 2B), 48.6 ppm (s, 2B); ^{11}B NMR (160 MHz, $CDCl_3$, 22 °C): δ = 91.8 (d, J_{B-H} = 155 Hz), 48.7 ppm (d, J_{B-H} = 131 Hz); ^1H NMR (500 MHz, $CDCl_3$, 22 °C): δ = 8.23 (br, 2H, B-H_t), 4.21 (br,

2H, B-H$_t$), 2.19 (s, 15H, C$_5$*Me*$_5$), 2.04 (s, 15H, C$_5$*Me*$_5$), -10.47 ppm (br, 2H, W-*H*-B); ^{13}C{^{1}H} NMR (22 °C, 125 MHz, $CDCl_3$): δ = 106.8 (*C*$_5$Me$_5$), 105.3 (*C*$_5$Me$_5$), 13.1 (C$_5$*Me*$_5$), 12.4 ppm (C$_5$*Me*$_5$); IR (CH_2Cl_2, cm^{-1}): 2495, 2451 (w, BH$_t$), 2036, 2011, 1993, 1765 (CO).

2: MS (ESI+): *m/z* calculated for [M-(H+2CO)]$^+$ 775.1532, found 775.1829; ^{11}B{^{1}H} NMR (160 MHz, $CDCl_3$, 22 °C): δ = 72.5 (s, 1B), 53.8 (s, 1B), 45.4 (s, 1B), 24.2 ppm (s, 1B); ^{1}H NMR (500 MHz, $CDCl_3$, 22 °C): δ = 5.80 (br, 4H, B-H$_t$), 2.17 (s, 30H, C$_5$*Me*$_5$), -9.65 (br, 2H, W-*H*-B), -13.03 ppm (br, 1H, *μ*$_3$-*H*); ^{13}C{^{1}H} NMR (22 °C, 125 MHz, $CDCl_3$): δ = 106.8 (*C*$_5$Me$_5$), 12.9 ppm (C$_5$*Me*$_5$); IR (CH_2Cl_2, cm^{-1}): 2471 (w, BH$_t$), 1994, 1934, 1803 (CO).

3: MS (ESI+): *m/z* calculated for [M-H]$^+$ 1018.9684, found 1018.9655; ^{11}B{^{1}H} NMR (160 MHz, $CDCl_3$, 22 °C): δ = 132.6 (s, 1B); ^{1}H NMR (500 MHz, $CDCl_3$, 22 °C): δ = 2.15 (s, 30H, C$_5$*Me*$_5$), -3.93 (br, 1H, W-*H*-B); ^{13}C{^{1}H} NMR (22 °C, 125 MHz, $CDCl_3$): δ = 101.5 (*C*$_5$Me$_5$), 10.6 ppm (C$_5$*Me*$_5$); IR (CH_2Cl_2, cm^{-1}): 2023, 1979 (CO).

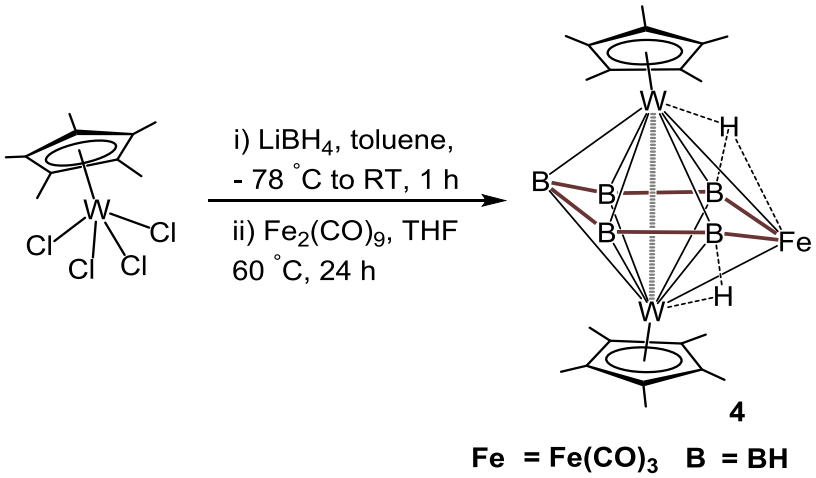

Scheme S3. Synthesis of compound **4**

Synthesis of 4: In a flame-dried Schlenk tube [Cp*WCl$_4$], (0.1 g, 0.21 mmol) in 10 mL of toluene was treated with 5-fold excess of [LiBH$_4$·THF] (0.7 mL) at -78 °C and allowed to stir at room temperature for 1 h. After removal of toluene, the residue was extracted into hexane and filtered through a frit using Celite. The brownish-green hexane extract was dried in vacuo, and taken in 10 mL of THF and heated at 60 °C in presence of [Fe$_2$(CO)$_9$] (0.02 g) for 24 h. The solvent was evaporated in vacuo and residue was extracted into hexane and passed through celite. After removal of solvent from the filtrate, the residue was subjected to chromatographic workup using silica gel TLC plates. Elution

with a hexane/CH_2Cl_2 (90:10 v/v) mixture yielded yellow **4** (0.005 g, 5 %) along with known [(μ_3-BH)$_2$H$_2${Cp*W(CO)$_2$}$_2${Fe(CO)$_2$}][4] (0.010 g, 10 %), [(μ_3-BH)$_2${Cp*W(CO)$_2$}$_2${Fe(CO)$_3$}][4] (0.020 g, 20 %), and [(Cp*W)$_2$B$_5$H$_9$][3] (0.015 g, 20 %).

4: MS (ESI$^+$): *m/z* calculated for [M]$^+$ 840.1627, found 840.1720; ^{11}B{^{1}H} NMR (160 MHz, $CDCl_3$, 22 °C): δ = 85.2 (s, 1B), 78.8 (s, 2B), 38.4 (s, 2B) ppm; ^{1}H NMR (500 MHz, $CDCl_3$, 22 °C): δ = 4.06 (br, B*H$_t$*), 2.27 ppm (s, 15H, C$_5$*Me$_5$*), 2.04 ppm (s, 15H, C$_5$*Me$_5$*), -10.6 (br, 2H, W-*H*-B) ; IR (CH_2Cl_2, cm^{-1}): 2487(w, BH_t), 1999, 1941 (CO).

I.3 X-ray Analysis Details

Suitable X-ray quality crystals of **1-4** were grown by slow diffusion of a hexane-CH_2Cl_2 solution. The crystal data of **1**, **2** and **4** were collected and integrated using a D8 VENTURE Bruker AXS diffractometer with graphite monochromated Mo-Kα (λ = 0.71073 Å) radiation at 150(2) K. The crystal data of **3** was collected and integrated using a Bruker AXS kappa apex3 CMOS diffractometer with graphite monochromated Mo-Kα (λ = 0.71073 Å) radiation at 296(2) K. The structures were solved by dual-space algorithm using SHELXT program[5] and refined with full-matrix least-squares methods based on F^2 (SHELXL program)[6]. The molecular structures were drawn using Olex2[7]. The non-hydrogen atoms were refined with anisotropic displacement parameters. Except the bridging hydrogen atoms were introduced through Fourier difference maps analysis. H atoms were finally included in their calculated positions and treated as riding on their parent atom with constrained thermal parameters. Crystallographic data have been deposited with the Cambridge Crystallographic Data Center as supplementary publication no CCDC- 2041472 (**1**), CCDC- 2041475 (**2**), CCDC- 2041477 (**3**), and CCDC- 2041478 (**4**). These data can be obtained free of charge from The Cambridge Crystallographic Data Centre via www.ccdc.cam.ac.uk/data_request/cif.

Crystal data for **1**: $C_{25}H_{34}B_4O_5W_2Co_2$, M_r = 943.32, Orthorhombic, space group *Pnma*, a = 16.5825(13) Å, b = 15.1254(14) Å, c = 11.4756(10) Å, V = 2878.3(4) Å^3, Z = 4, ρ_{calcd} = 2.177 g/cm^3, μ = 9.133 mm^{-1}, F(000) = 1784, R_1 = 0.0292, wR_2 = 0.0838, 3439 independent reflections [2θ≤55.04°] and 196 parameters.

Crystal data for **2**: $C_{23}H_{34}B_4O_3W_2Co$, M_r = 828.37, Orthorhombic, space group *Pbcn*, a = 27.3391(14) Å, b = 11.5763(5) Å, c = 17.1383(8) Å, V = 5424.0(4) Å^3, Z = 8, ρ_{calcd} = 2.029 g/cm^3, μ = 9.088 mm^{-1},

F(000) = 3128, R_1 = 0.0531, wR_2 = 0.1202, 4999 independent reflections [2θ≤54.96°] and 314 parameters.

Crystal data for **3**: $C_{29}H_{31}BO_9W_2Co_2$, M_r = 1019.91, Monoclinic, space group $P2_1/n$, a = 9.0186(7) Å, b = 16.7708(13) Å, c = 21.9213(17) Å, β = 101.710(2)°, V = 3246.6(4) Å^3, Z = 4, ρ_{calcd} = 2.087 g/cm^3, μ = 8.116 mm^{-1}, F(000) = 1936, R_1 = 0.0554, wR_2 = 0.1103, 6362 independent reflections [2θ≤51.98°] and 393 parameters.

Crystal data for **4**: $C_{23}H_{30}B_5O_3W_2Fe$, M_r = 832.07, Orthorhombic, *Pbca*, a = 15.6231(13) Å, b = 15.1720(12) Å, c = 22.868(2) Å, V = 5420.5(8) Å^3, Z = 8, ρ_{calcd} = 2.039 g/cm^3, μ = 9.018 mm^{-1}, F(000) = 3128, R_1 = 0.0356, wR_2 = 0.0702, 6183 independent reflections [2θ≤54.94°] and 317 parameters.

I.4 Spectroscopic details

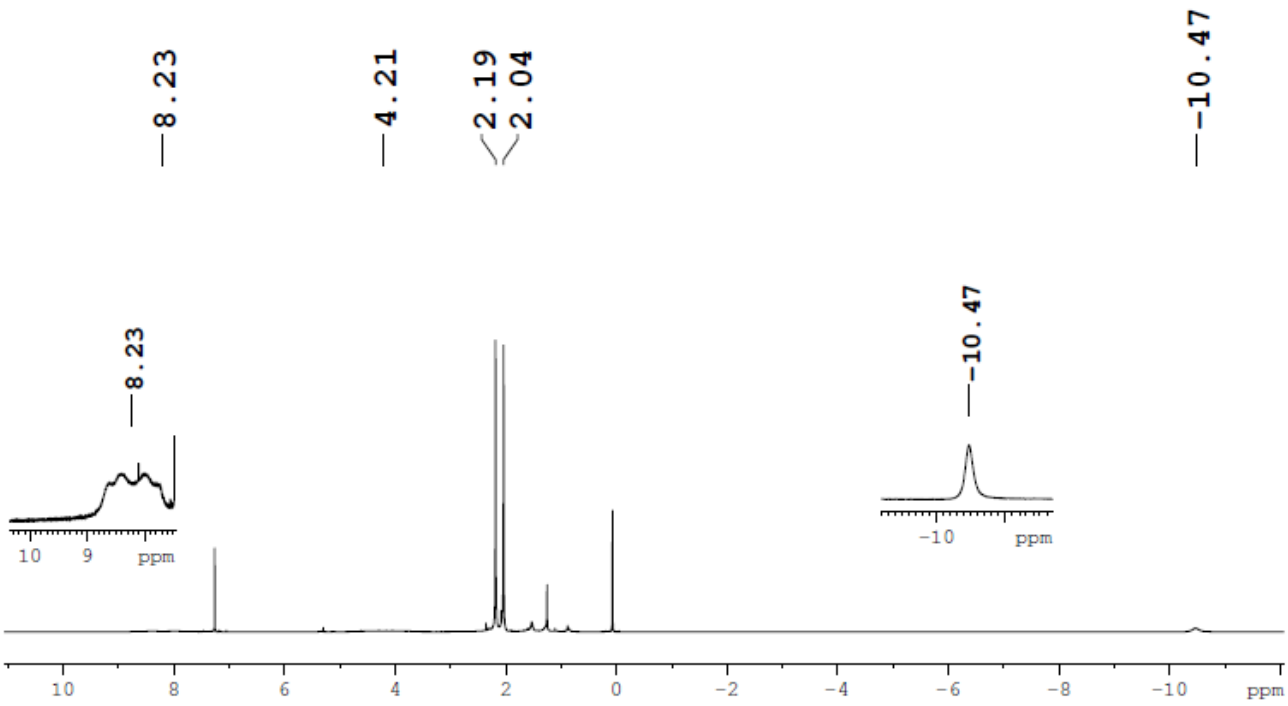

Figure S6. ^{1}H NMR spectrum of compound **1**.

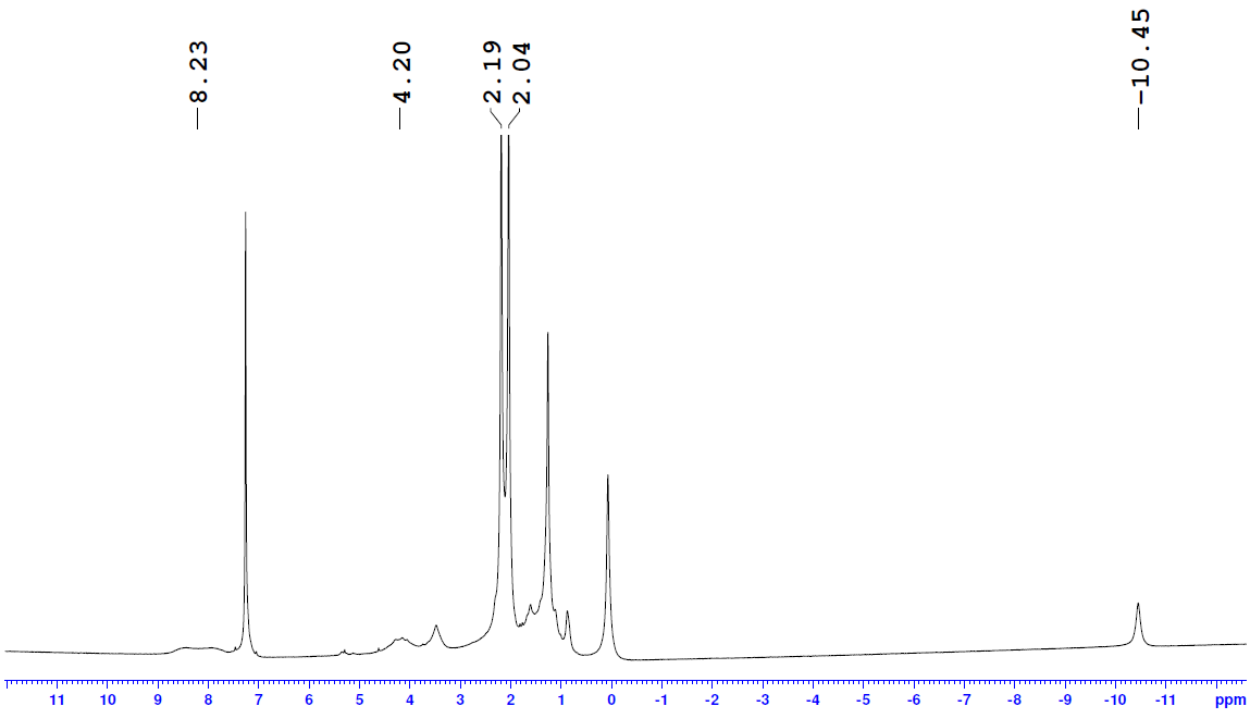

Figure S7. ^{1}H{^{11}B} NMR spectrum of compound **1**.

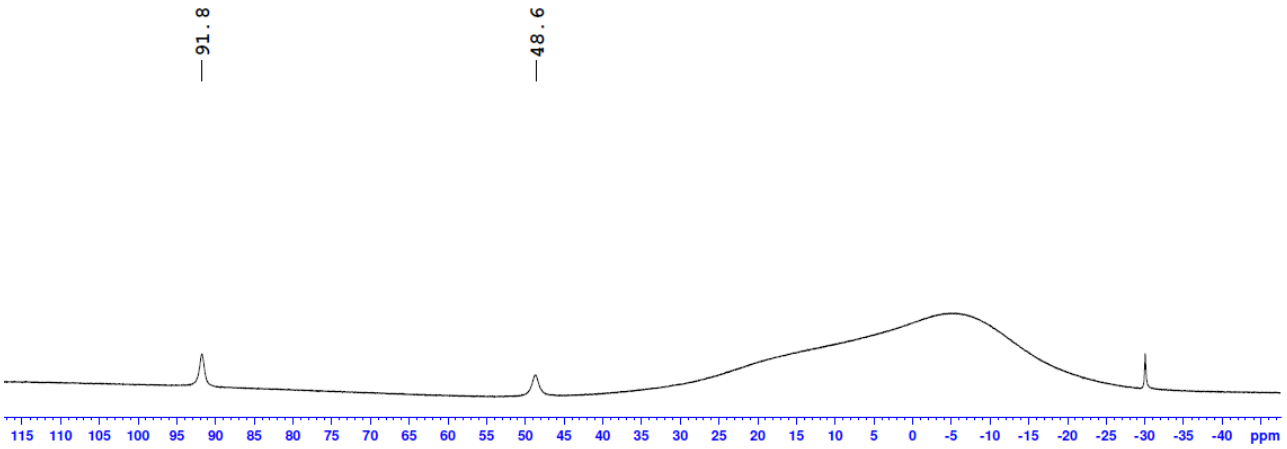

Figure S8. $^{11}B\{^{1}H\}$ NMR spectrum of compound **1**.

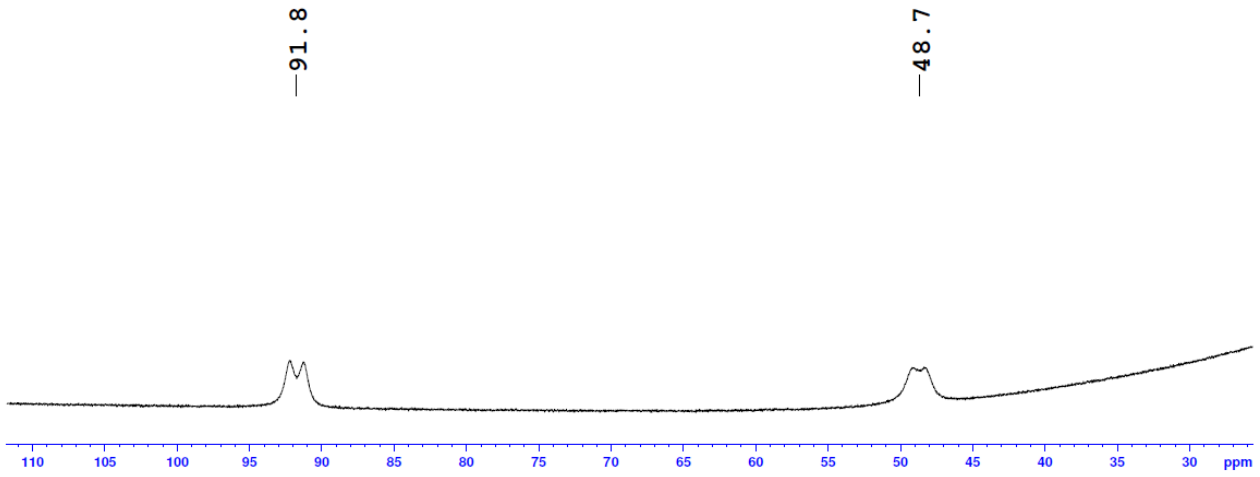

Figure S9. ^{11}B NMR spectrum of compound **1**.

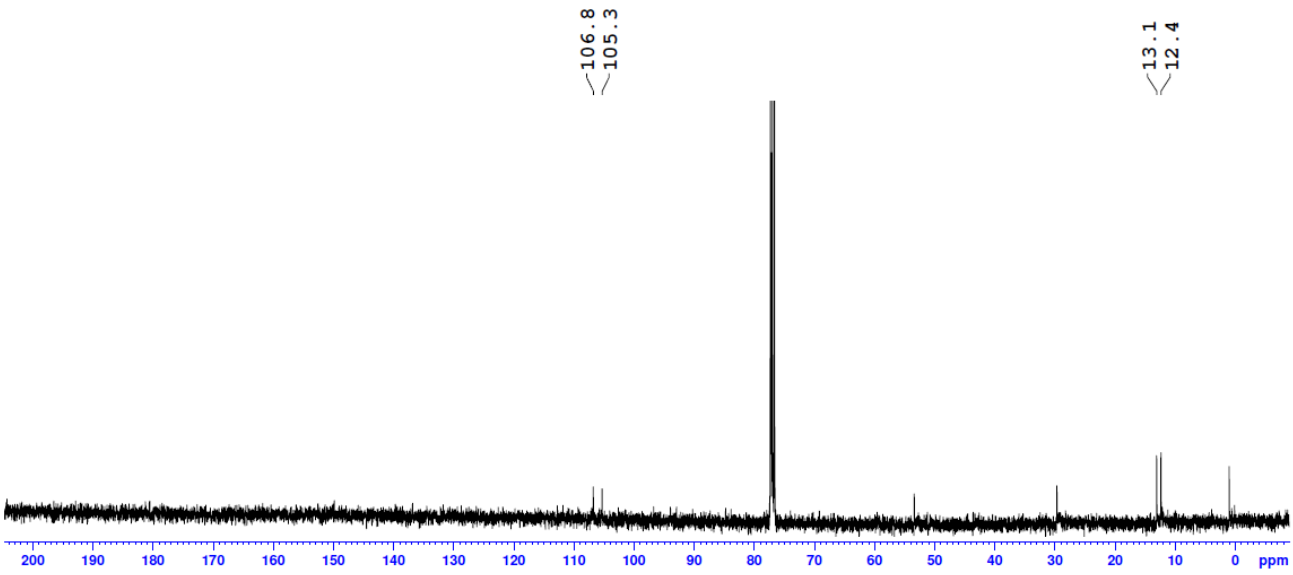

Figure S10. $^{13}C\{^{1}H\}$ NMR spectrum of compound **1**.

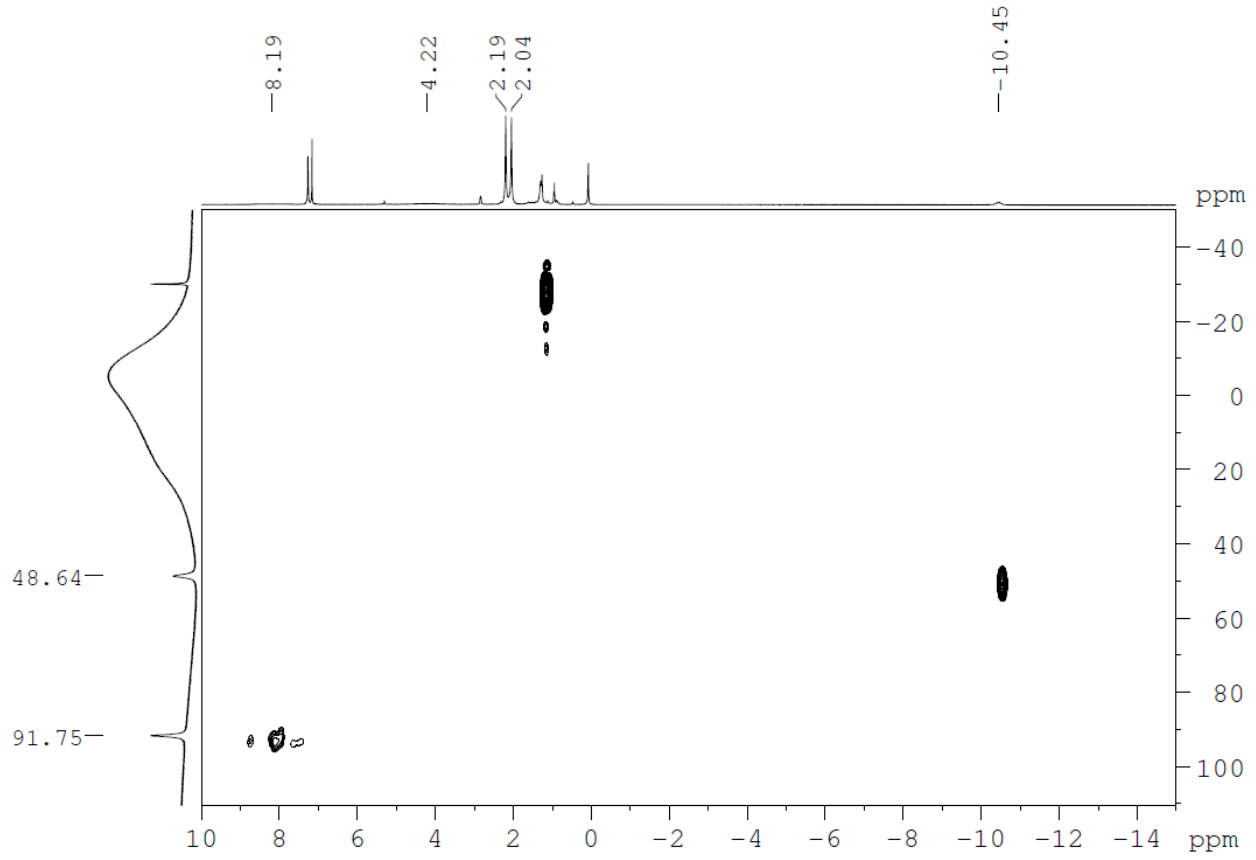

Figure S11. ^{1}H-$^{11}B\{^{1}H\}$ HSQC NMR spectrum of compound **1**.

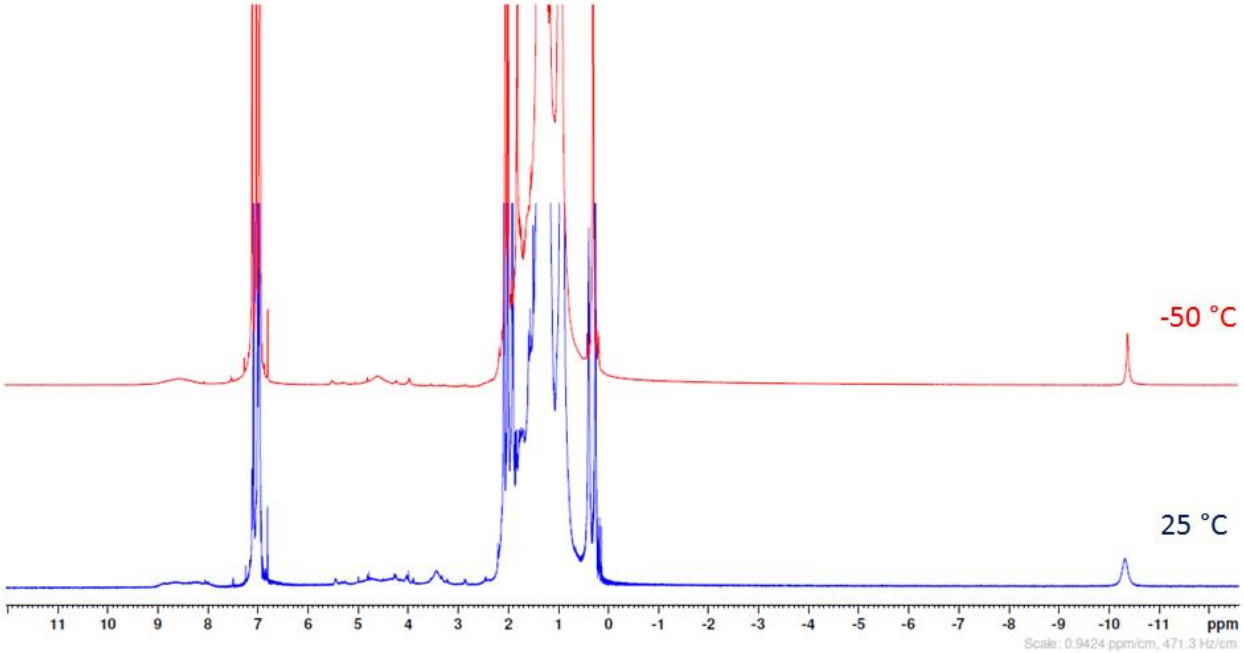

Figure S12. Stacked plot of ^{1}H NMR spectrum of compound **1** at -50 °C and 25 °C in d_8-toluene.

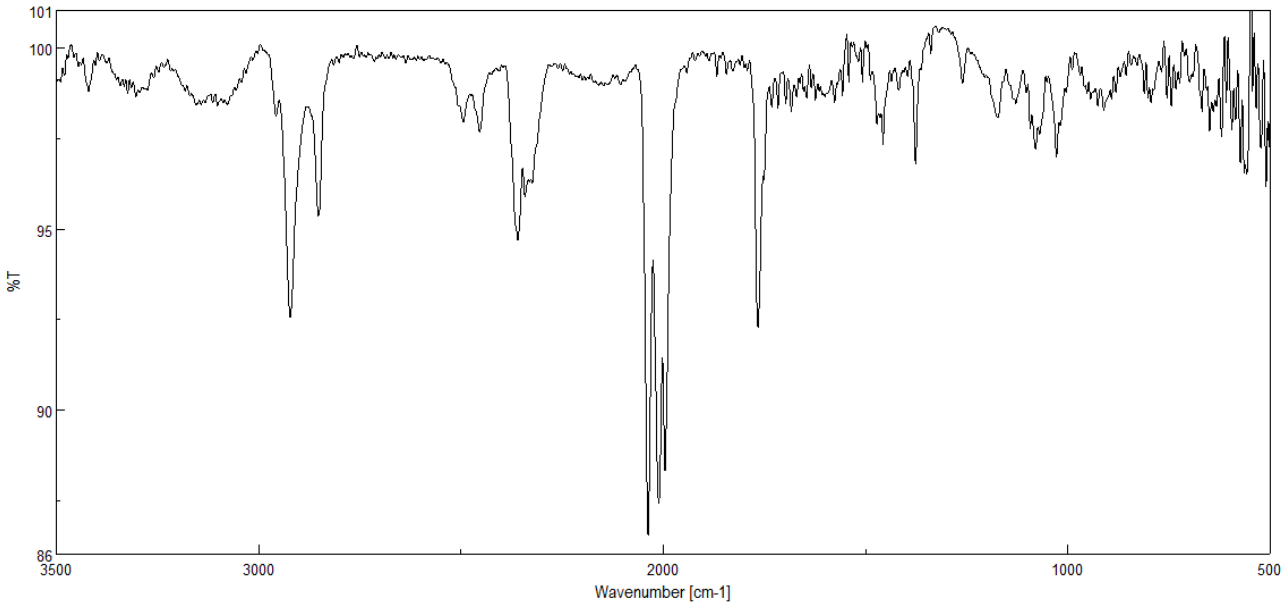

Figure S13. IR spectrum of compound **1**.

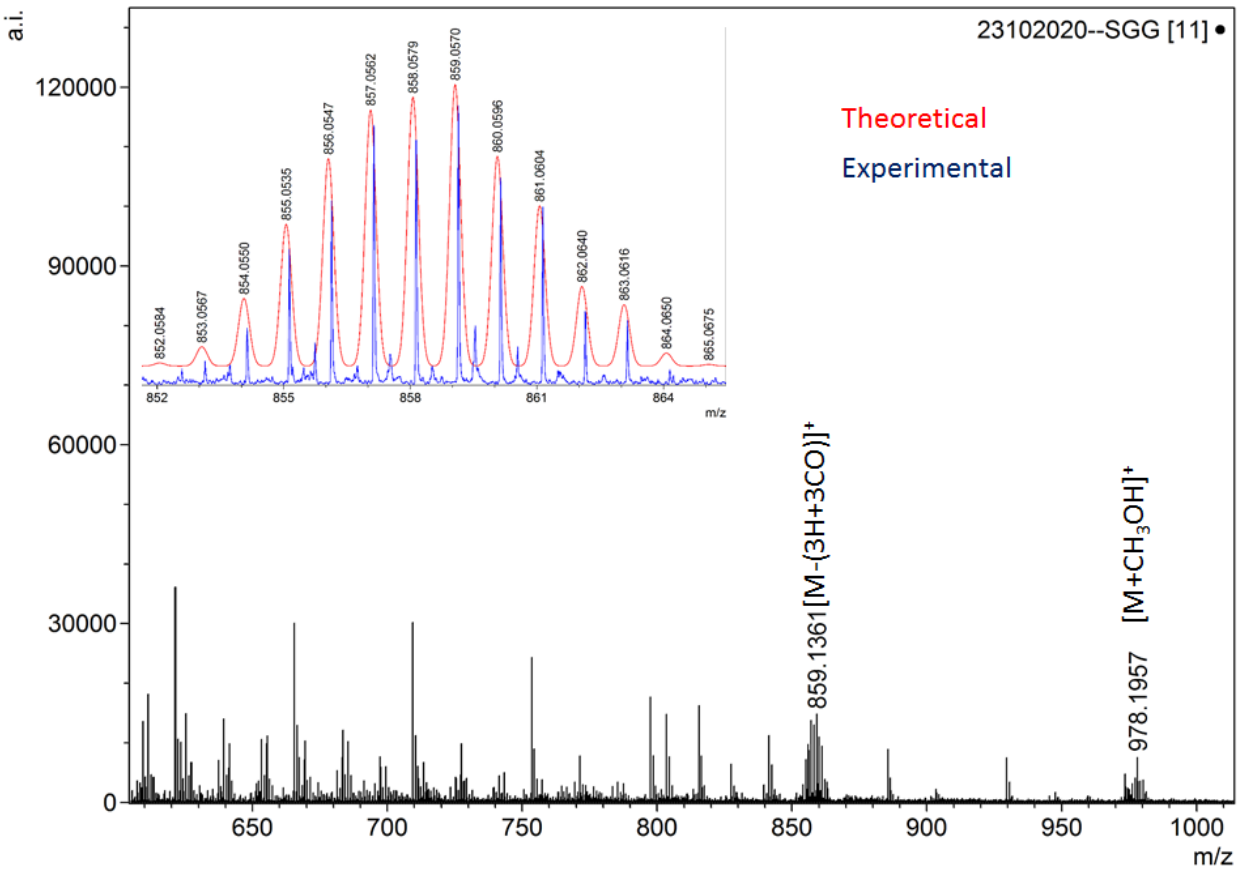

Figure S14. ESI-MS spectrum of compound **1** in CH_2Cl_2 and MeOH mixture.

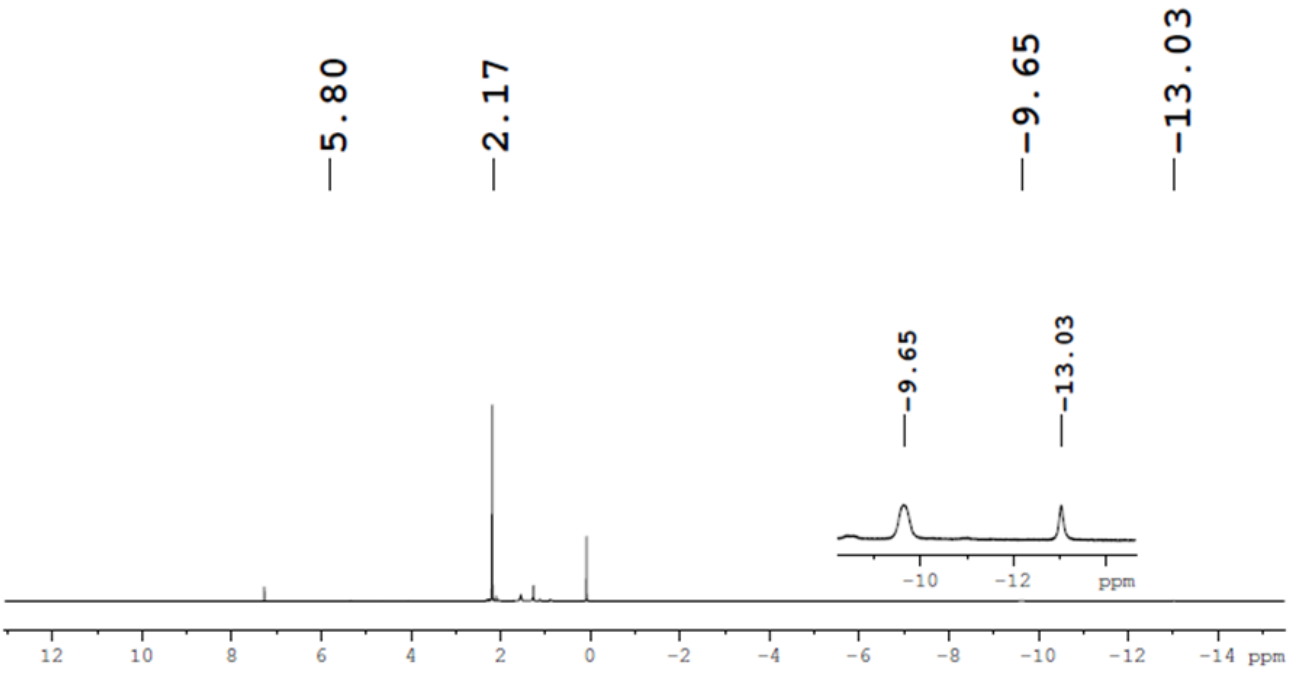

Figure S15. ^{1}H NMR spectrum of compound **2**.

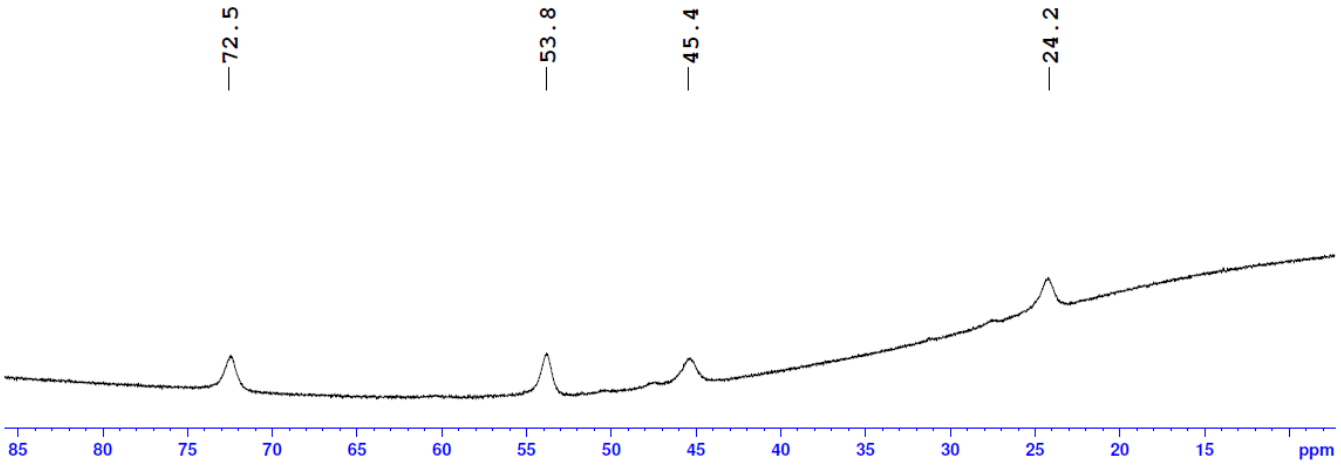

Figure S16. $^{11}B\{^{1}H\}$ NMR spectrum of compound **2**.

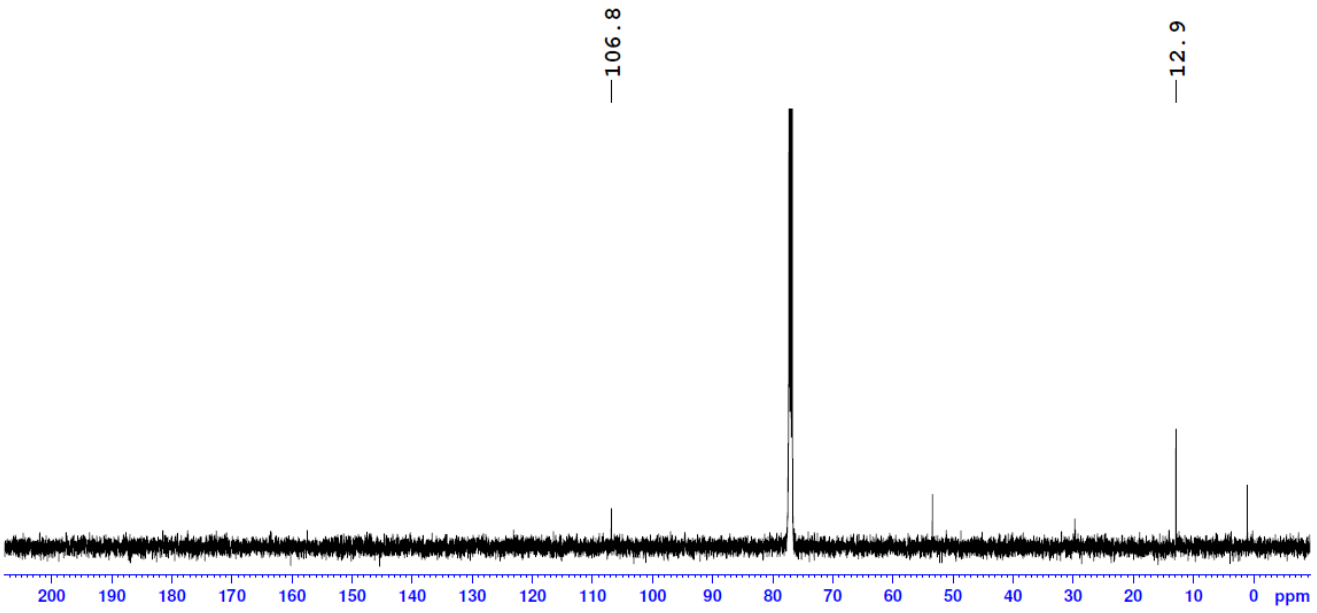

Figure S17. $^{13}C\{^{1}H\}$ NMR spectrum of compound **2**.

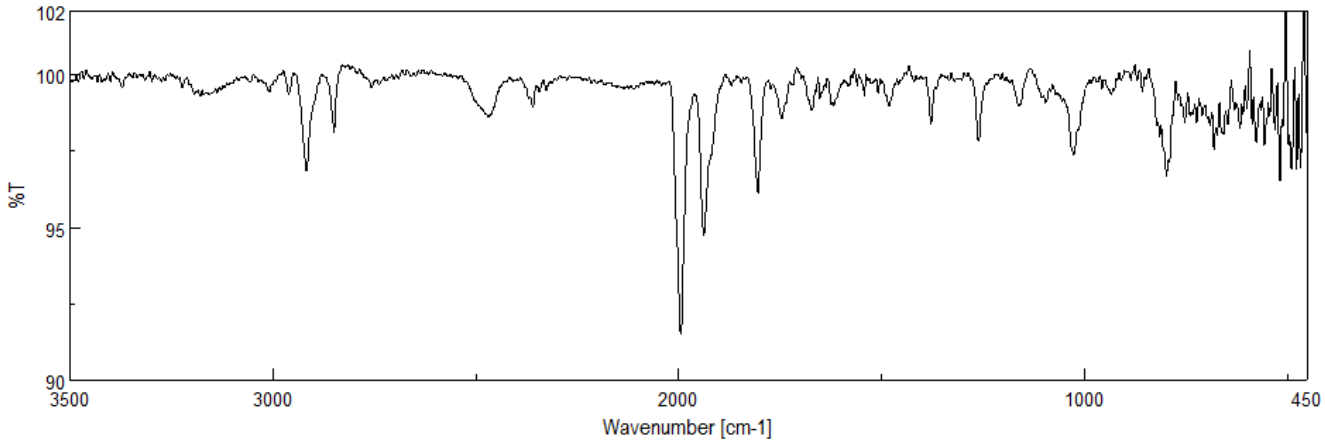

Figure S18. IR spectrum of compound **2**.

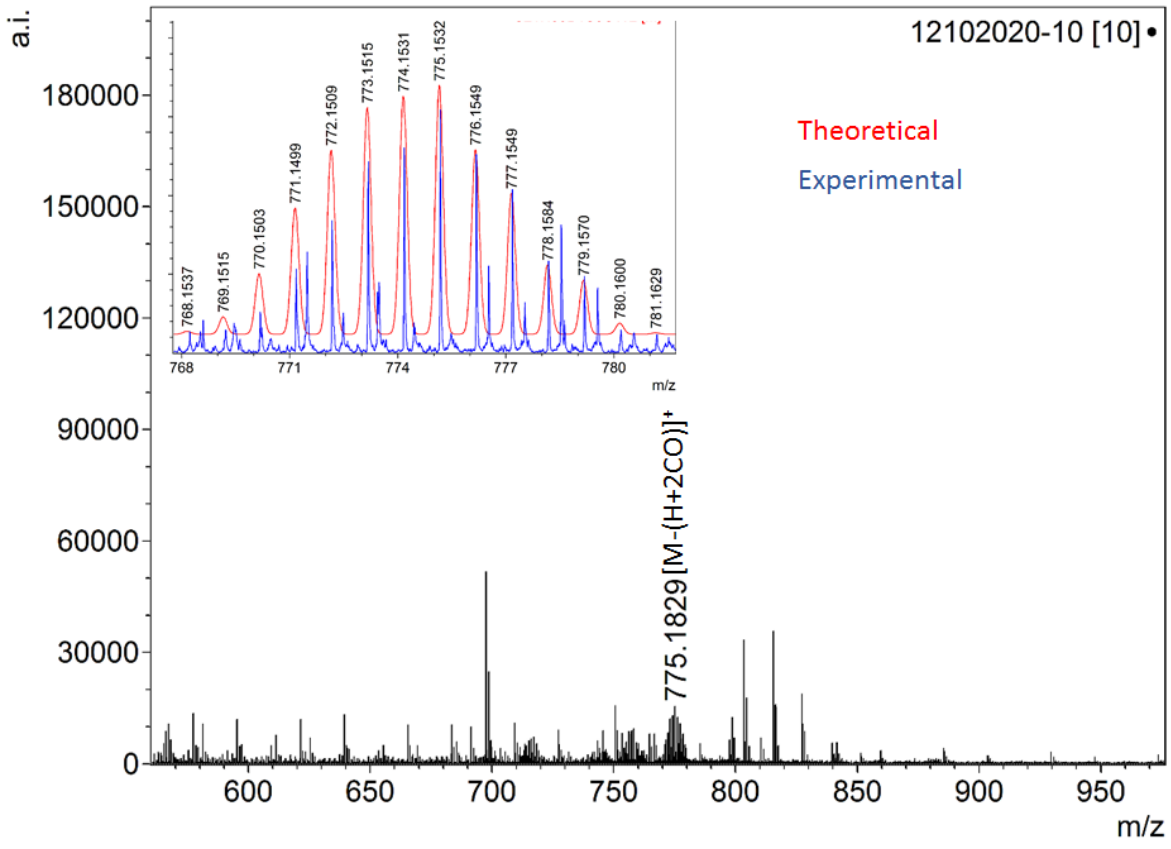

Figure S19. ESI-MS spectrum of compound **2** in CH_2Cl_2 and MeOH mixture.

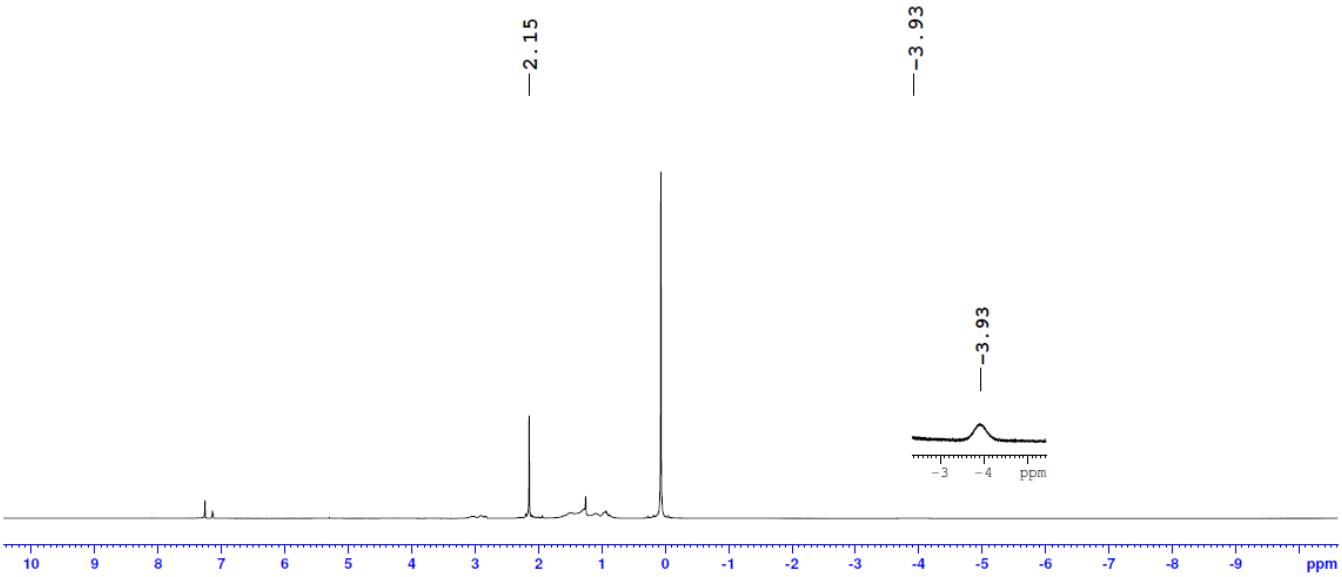

Figure S20. ^{1}H NMR spectrum of compound **3**.

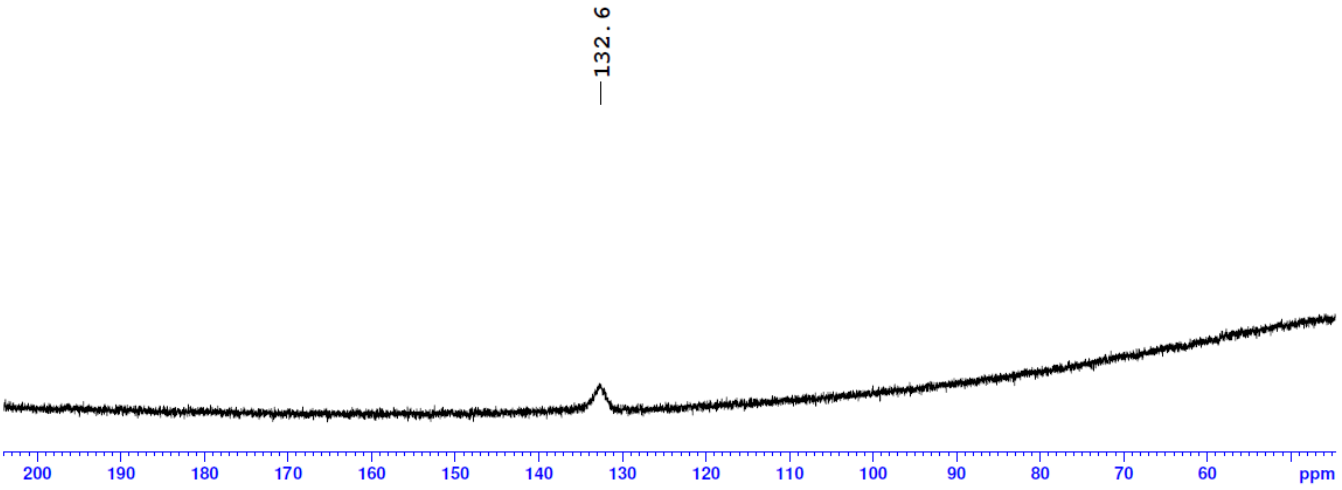

Figure S21. ^{11}B{^{1}H} NMR spectrum of compound **3**.

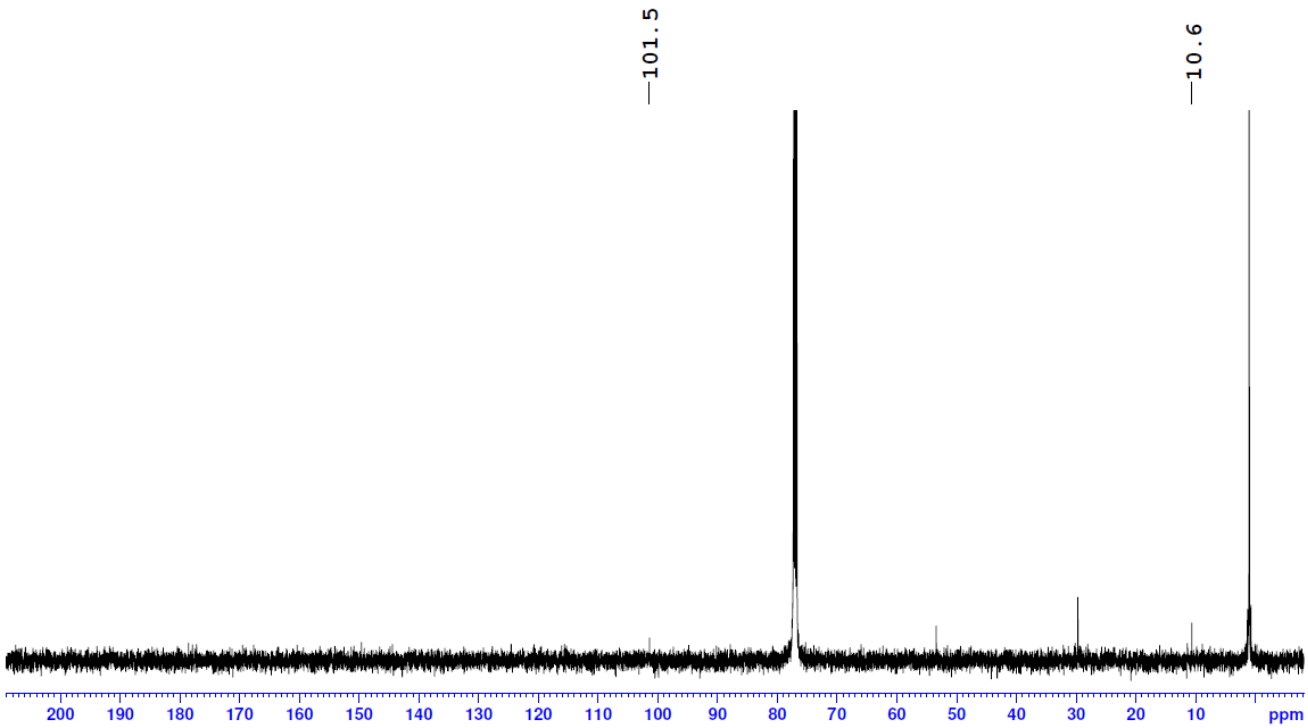

Figure S22. $^{13}C\{^{1}H\}$ NMR spectrum of compound **3**.

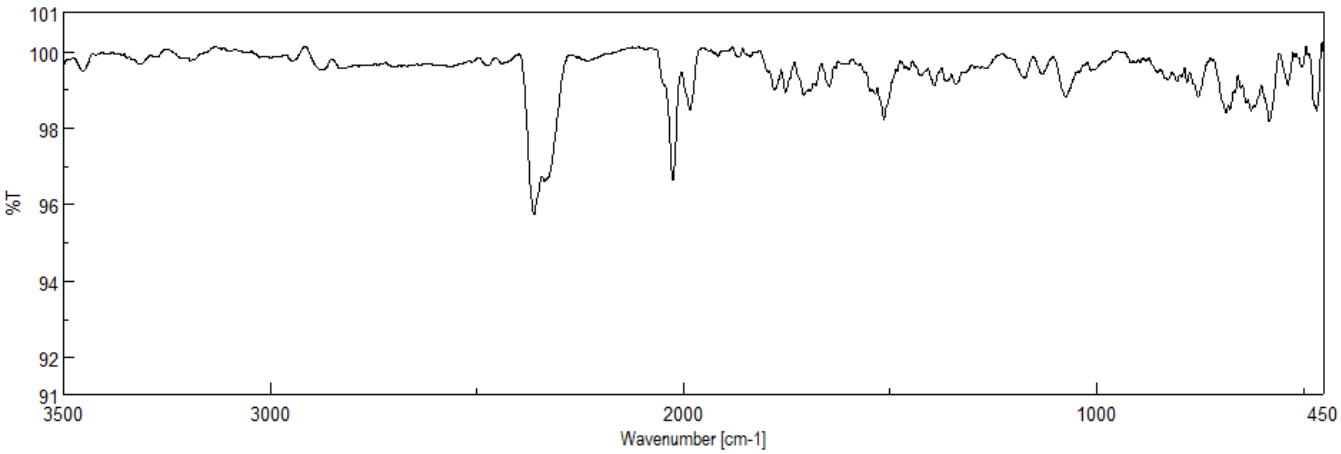

Figure S23. IR spectrum of compound **3**.

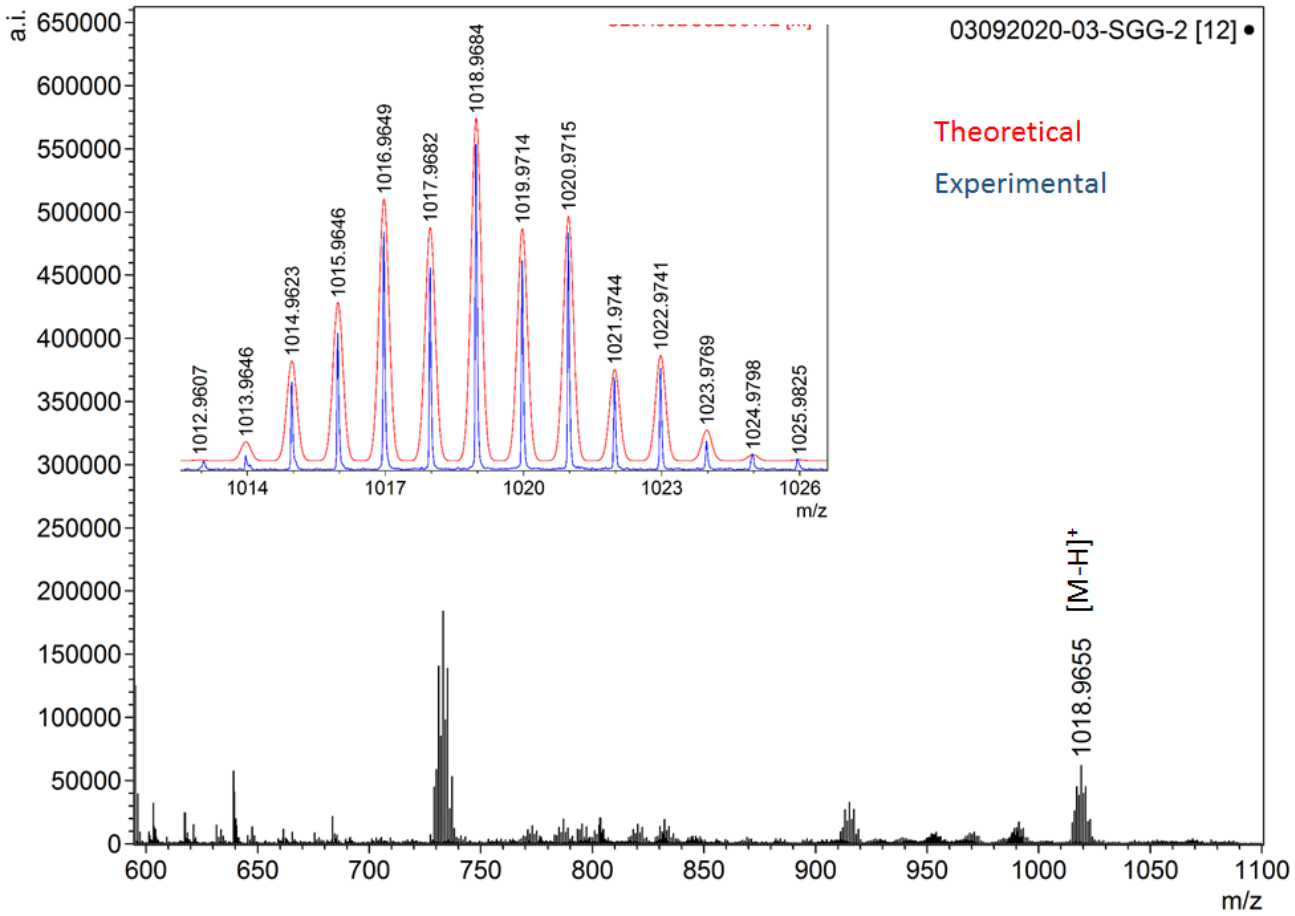

Figure S24. ESI-MS spectrum of compound **3** in CH_2Cl_2 and MeOH mixture.

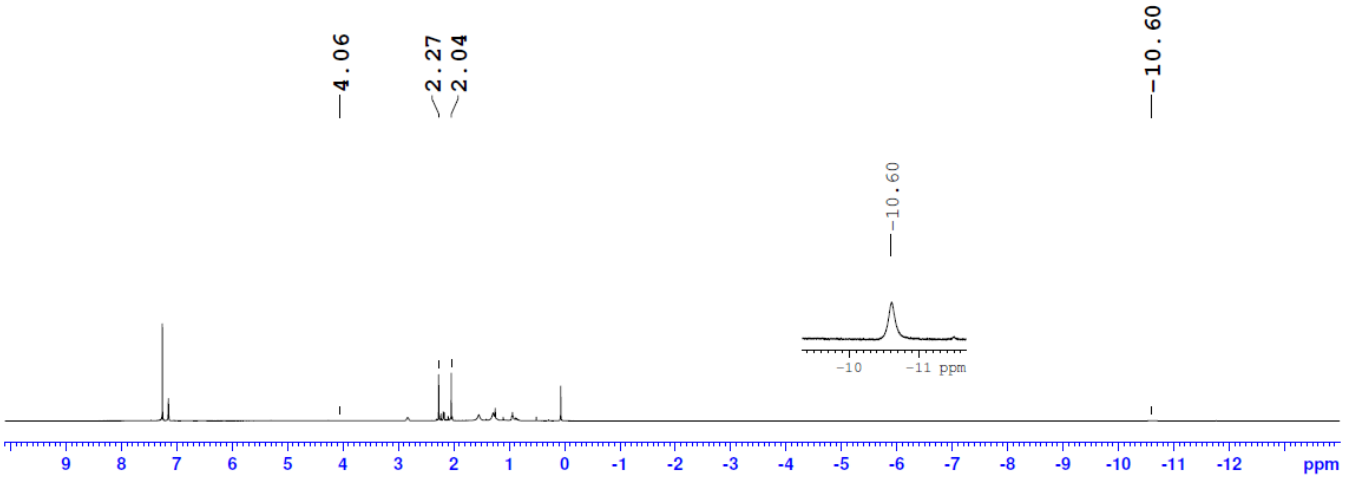

Figure S25. ^{1}H NMR spectrum of compound **4**.

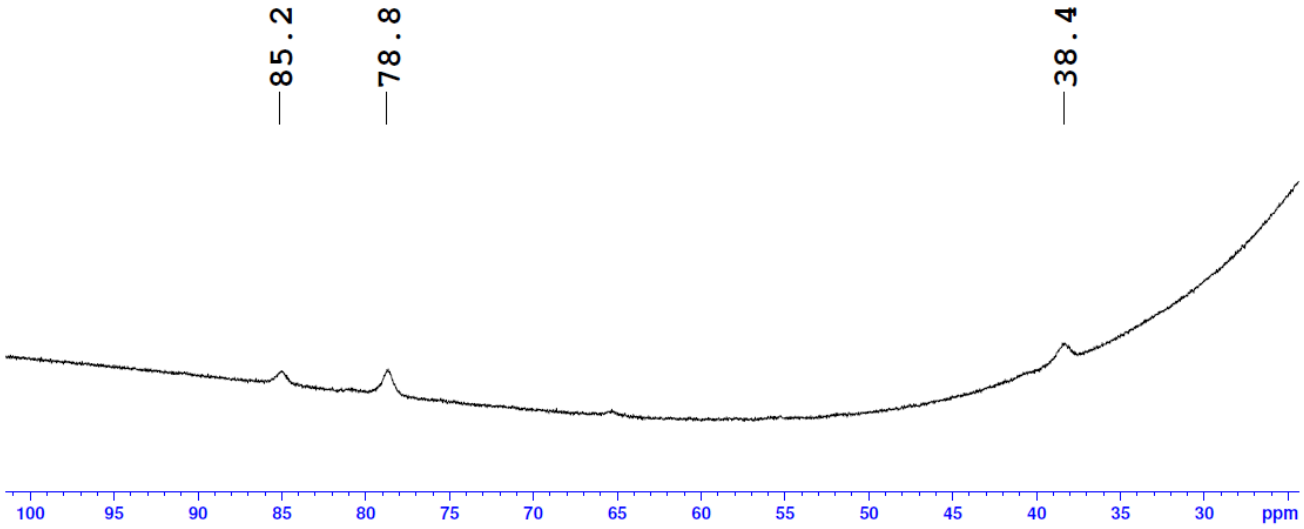

Figure S26. $^{11}B\{^{1}H\}$ NMR spectrum of compound **4**.

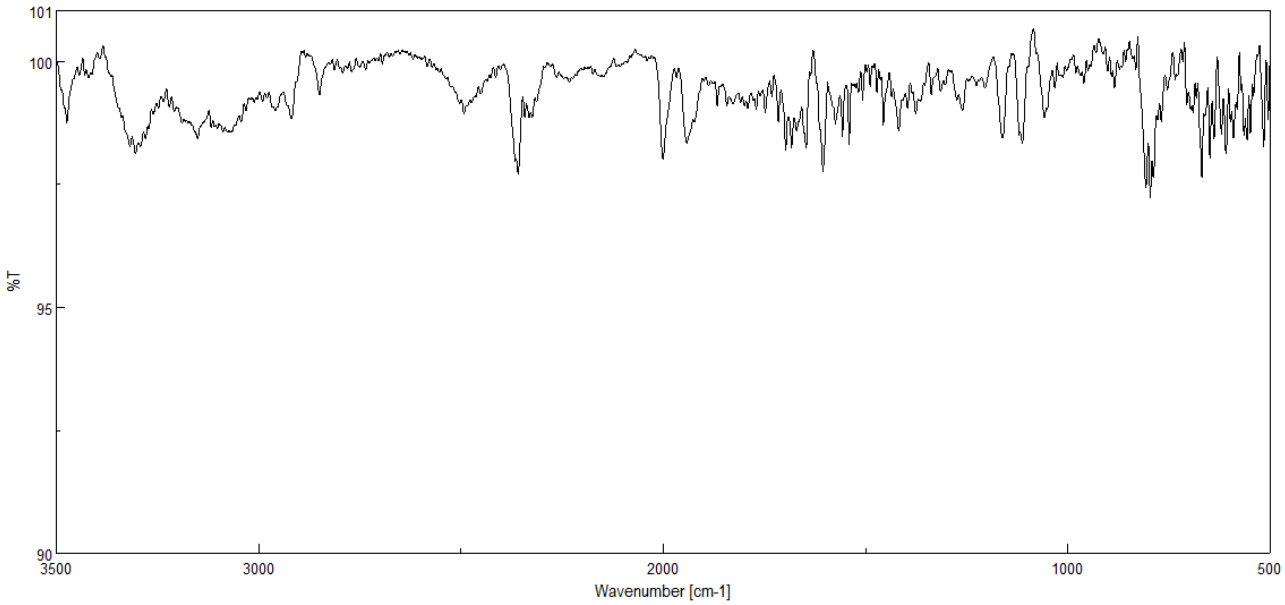

Figure S27. IR spectrum of compound **4**.

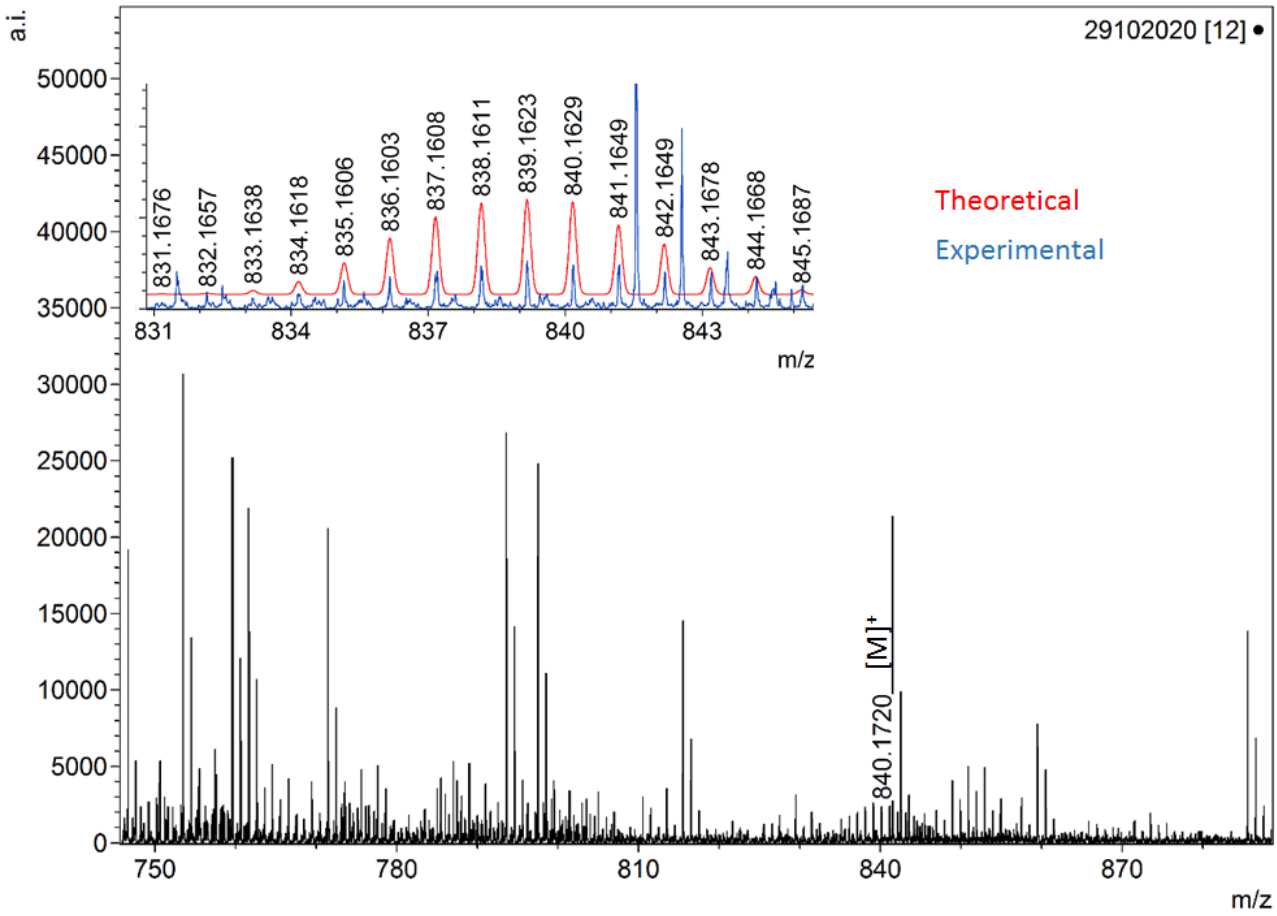

Figure S28. ESI-MS spectrum of compound **4** in CH_2Cl_2 and MeOH mixture.

II Computational details

Quantum chemical calculations were performed on compounds **1'**, **2'**, **4'** (Cp analogues of **1**, **2** and **4**), **II**-**IV** using density functional theory (DFT) as implemented in the Gaussian 16 program package.[8] Geometry optimizations were conducted in the gas phase (no solvent effect) without any symmetry constraints using the B3LYP functional[9] (molecules were optimised using BP86 functional[10] also. However, optimisation using the hybrid functional, B3LYP produced geometry having slightly better corroboration with experimental results, apart from the case of **IV**, due the loss of planarity using B3LYP functional) and the triple-ζ quality def2-TZVP basis set.[11] The core electrons of W was replaced by quasi-relativistic effective core potentials def2-ECP.[12] The optimized geometries were characterized as true minima by analyzing analytical frequencies. The gauge including atomic orbital (GIAO) method[13] was employed to compute the NMR chemical shifts of the B3LYP/def2-TZVP optimized geometries. The ^{11}B NMR chemical shifts were calculated relative to B_2H_6 (B3LYP/ def2-TZVP B shielding constant, 84.2 ppm) and converted to the usual [$BF_3{\cdot}OEt_2$] scale by using the

experimental δ (^{11}B) value of B_2H_6 (δ = 16.6 ppm).[14] TMS (SiMe4) was used as internal standard for the ^{1}H NMR chemical shift calculations (B3LYP H shielding constant 31.92 ppm). Wiberg bond indices (WBIs)[15] were obtained from a natural bond orbital (NBO)[16] analysis. All the optimized structures and orbital graphics were generated with Chemcraft.[17]

Table S1. Experimental and calculated (in parenthesis) bond lengths in Å and Wiberg bond indices (WBI) for the compounds **1′**, **2′** and **4′** optimized at the B3LYP/def2-TZVP level.

atom pair	**1′**		**2′**		**4′**	
	distance	**WBI**	**distance**	**WBI**	**distance**	**WBI**
W-W	2.790(2.803)	0.7644	2.833(2.858)	0.7211	2.812(2.813)	0.7024
W-B	2.251(2.256)	0.6096	2.253(2.267)	0.5943	2.267(2.272)	0.5961
W-M‘	2.734(2.778)	0.3577	2.670(2.709)	0.3965	2.722(2.764)	0.6184
M’-M‘	2.515(2.536)	0.2670	--	--	--	
B-B	1.714(1.728)	0.5618	1.731(1.731)	0.5842	1.729(1.763)	0.5592
B-M‘	2.126(2.149)	0.3466	2.130(2.205)	0.2804	2.235(2.243)	0.3769

Table S2. DFT calculated (B3LYP/def2-TZVP) and experimental NMR chemical shifts δ (ppm) for compounds **1′**, **2′** and **4′**.

Compound	**1′**		**2′**		**4′**		
	Exp.	Calc.	Exp.	Calc.	Exp.	Calc.	Calc*
B1	48.6	38.69	24.2	17.41	38.4	28.42	30.28
B2	48.6	38.77	45.4	33.91	38.4	35.48	34.75
B3	91.8	98.45	53.8	44.88	78.8	76.03	78.37
B4	91.8	98.99	72.5	63.64	78.8	79.45	79.56
B5	--	--	--	--	85.2	80.28	84.02

μ_3-H	-10.47	-10.71	-13.03	-13.04	-10.60	-18.36	-19.17
μ-H			-9.65	-9.69	-10.60	-10.19	-9.56
			-9.65	-8.93			

*Calculated using BP86/def2-TZVP optimised geometry

Table S3. Calculated energies of the HOMO and LUMO (eV) and HOMO-LUMO gaps ($\Delta E = E_{LUMO}-E_{HOMO}$, eV) for compounds **1′**, **2′** and **4′**.

	1′	**2′**	**4′**
HOMO (eV)	-5.87	-5.59	-5.80
LUMO (eV)	-2.60	-2.64	-2.55
ΔE (eV)	3.27	2.95	3.25

Table S4. Calculated natural charges (q), natural valence population (Pop) for compounds **1′** and **4′**.

	1′		**4′**	
	q	pop	q	pop
W	-0.15034	6.10115	-0.24459	6.20252
	-0.25702	6.21087	-0.25291	6.21617
Co	-1.19914	10.19353	-1.87765	9.86041
	-1.1995	10.19385		
B	-0.06939	3.02556	-0.11287	3.07428
	-0.08924	3.0395	-0.07635	3.0341
	-0.06882	3.02498	0.00193	2.95889
	-0.08909	3.03933	-0.01891	2.9713
			-0.0676	3.02689

$[(CpW)_2B_4H_{10}] + Co_2(CO)_8 \longrightarrow [(CpW)_2\{\mu\text{-}\eta^6\text{:}\eta^6\text{-}B_4H_4(H)_2Co_2(CO)_5\}] + 3CO + 2H_2$ pathway 1

I′ **1′**

$[(CpW)_2(\mu\text{-}H)_2(\mu_3\text{-}H)B_4H_4Co(CO)_3] + Co_2(CO)_8 \longrightarrow [(CpW)_2\{\mu\text{-}\eta^6\text{:}\eta^6\text{-}B_4H_4(H)_2Co_2(CO)_5\}] + Co(CO)_4H + 2CO$

2′ **1′** pathway 2

ΔG of the reaction = Σ(G of the products)- Σ(G of the reactant)

ΔG of reaction pathway 1 = 2.2973 kJ/mol
ΔG of reaction pathway 2 = 7.59294658 kJ/mol

Scheme S4. Calculated change in free energy of the reaction pathways for the formation of **1′**.

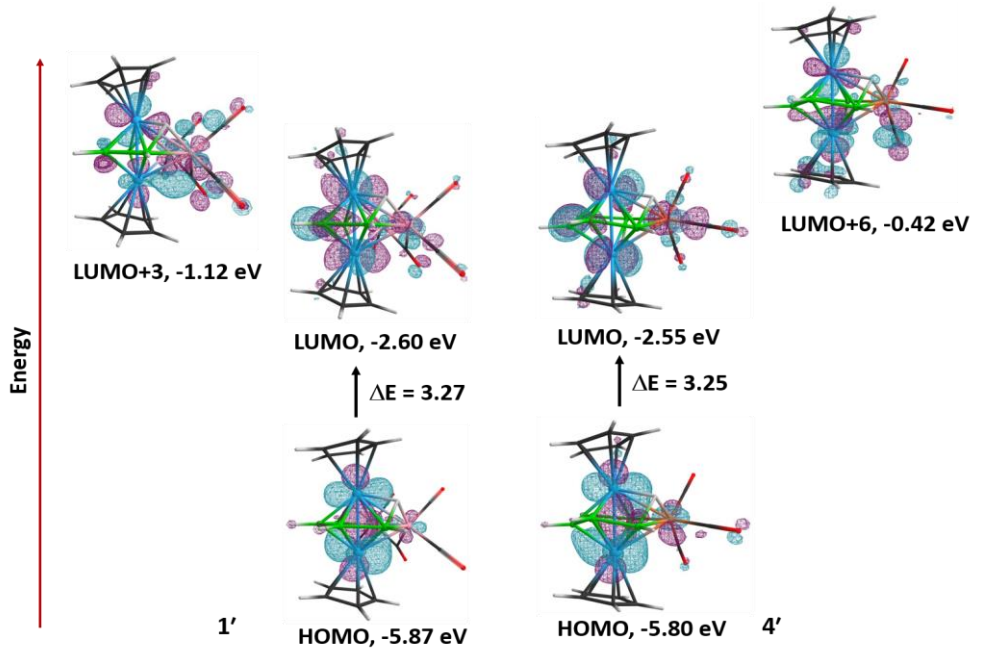

Figure S29. Frontier molecular orbitals of **1′** and **4′** as obtained from calculation. Isocontour value: ±0.04 $(e/bohr^3)^{1/2}$.

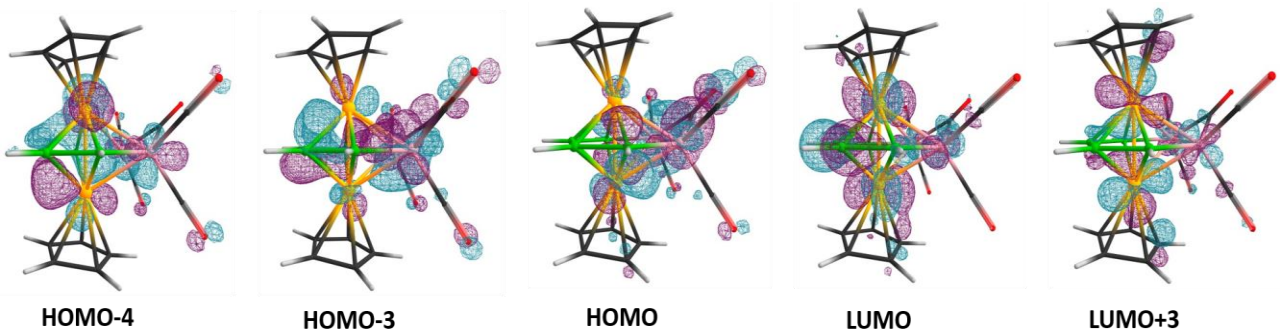

Figure S30. Selected DFT-calculated molecular orbitals of $[(CpRe)_2\{\mu\text{-}\eta^6\text{:}\eta^6\text{-}B_4H_4Co_2(CO)_5\}]$, **IV**. Isocontour value: ±0.04 $(e/bohr^3)^{1/2}$.

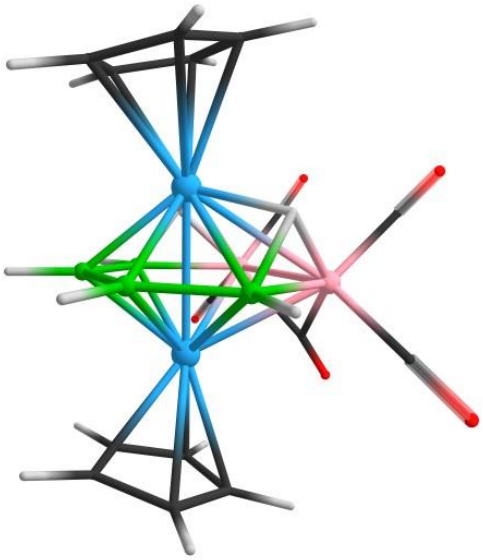

T.E = -3957.287399 a.u.

Figure S31. Optimized geometry of **1'**

W	1.288888788	-0.766125718	0.000334458
C	2.955184357	-2.479941970	-0.003342771
C	3.188283490	-1.684838611	1.150281238
C	3.554416847	-0.387034734	0.716900327
W	-1.513987466	-0.719663538	-0.000368297
C	-3.729220513	-0.155935607	-0.703148434
C	-3.454343995	-1.480332925	-1.151028585
C	-3.291243454	-2.305119783	-0.008574701
Co	0.074992303	1.287097635	-1.268015339
C	-1.054765999	2.652685151	-1.533505671
O	-1.783903884	3.505450552	-1.738210349
C	1.067097819	1.505715885	-2.719258158
O	1.721515135	1.648132189	-3.641583029
C	1.373005386	1.890700499	0.001376717
O	2.311937713	2.590302065	0.002673971
B	-0.146757481	-2.218785763	-0.864634630
H	-0.166050911	-3.269711692	-1.420544998
B	-0.042167349	-0.786174238	-1.823762451
H	-0.019956124	-1.043608619	-2.985558782
C	3.192216034	-1.676314010	-1.150221658
C	3.556812025	-0.381768509	-0.705958328
C	-3.727984974	-0.164597279	0.712797362
C	-3.452247860	-1.494266188	1.144182507
B	-0.148656719	-2.219002985	0.864075474
H	-0.168149518	-3.270032225	1.419776828
B	-0.041884195	-0.786491888	1.823465069

H	-0.019675878	-1.043871922	2.985274227
Co	0.072149420	1.286997128	1.268252342
C	-1.060422681	2.650927812	1.529355180
O	-1.791770691	3.502482709	1.731273211
C	1.061044999	1.508746658	2.721357626
O	1.713257250	1.653172031	3.644913808
H	2.656646027	-3.514214161	-0.007683484
H	3.095625427	-2.010856919	2.172781935
H	3.796699746	0.451834736	1.348326146
H	3.801032781	0.461823805	-1.330288960
H	3.103080809	-1.994749447	-2.175434531
H	-3.074046637	-3.359480612	-0.015155539
H	-3.392730332	-1.803126475	-2.177002378
H	-3.388834026	-1.829446830	2.166046022
H	-3.912336055	0.683922843	1.351488499
H	-3.914776467	0.700208320	-1.331233070
H	-1.125382628	0.076285361	1.675765110
H	-1.124615078	0.077069877	-1.675986037

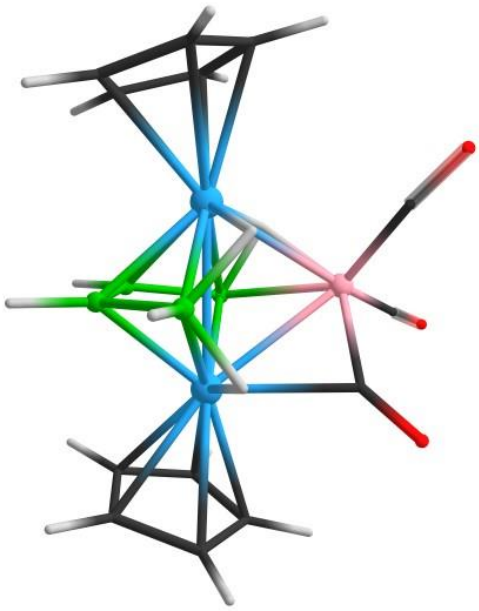

T.E = -2348.249629 a.u.

Figure S32. Optimized geometry of **2'**

W	-1.403613802	-0.519166799	-0.116956747
C	-3.629827140	-0.836990997	-0.939847264
C	-3.705294510	0.148001974	0.081250265
C	-3.326493274	-0.451082576	1.307274973
C	-3.008139024	-1.812151529	1.040607661
C	-3.206967765	-2.054031645	-0.345740925

W	1.451130474	-0.442870203	0.006573867
C	3.176073794	-1.585424690	1.165384311
C	3.246644602	-1.995433720	-0.195259208
C	3.593928835	-0.861717429	-0.974085630
C	3.752785813	0.248807096	-0.102317976
C	3.497788140	-0.201511509	1.218567646
Co	0.061662776	1.808837573	0.184629600
C	1.366808847	2.481709469	-0.788669748
O	2.158645399	3.034217926	-1.411626324
C	-0.588097892	3.198663810	1.101790578
O	-0.968059545	4.097935233	1.693279015
C	-1.328520196	1.647279864	-0.988931322
O	-1.956122100	2.234641078	-1.776072965
B	0.126892448	-1.184064512	-1.742979681
H	0.239000224	-1.738818823	-2.792392607
B	0.064858037	-2.176975760	-0.324598023
H	0.120908100	-3.362306032	-0.430274676
B	0.073490468	-1.551953758	1.264923309
H	0.043089195	-2.302354038	2.185919131
B	-0.201336422	0.145601074	1.607621432
H	-0.362522469	0.380445820	2.763806140
H	-3.291313978	0.033431550	2.268135357
H	-3.995755769	1.175936434	-0.059591716
H	-3.854427062	-0.680657814	-1.982646623
H	-3.057539842	-2.992633358	-0.852176977
H	-2.686210975	-2.538959595	1.766328875
H	4.023799930	1.249267240	-0.394475997
H	3.536433668	0.402963098	2.110125841
H	2.947288709	-2.216874555	2.006003353
H	3.719238896	-0.844695278	-2.044344187
H	3.063194445	-2.989002403	-0.566140968
H	0.984673202	0.834128768	1.341960964
H	-0.946114458	-0.440842898	-1.901228486
H	1.095755487	-0.271002147	-1.785286624

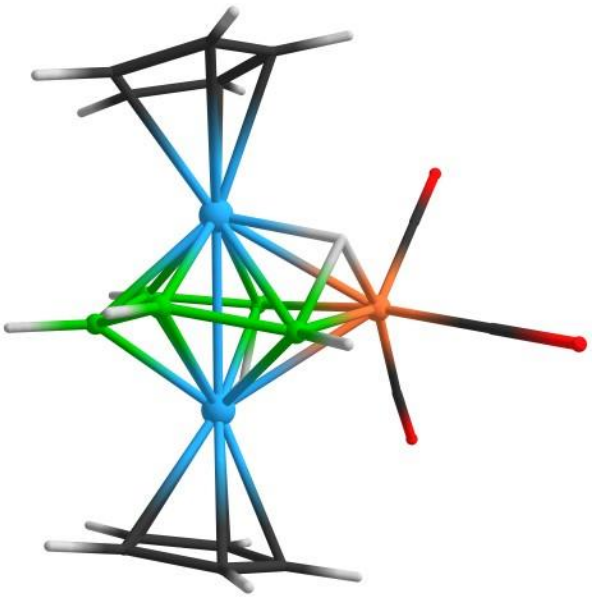

T.E = -2254.042847 a.u.

Figure S33. Optimized geometry of **4'**

W	1.390605149	-0.580570229	-0.090421267
W	-1.419404647	-0.534902100	0.037239446
Fe	-0.017935600	1.821154348	0.062707811
O	2.222988859	2.879658777	-1.480744424
O	0.508419223	3.711386054	2.248247246
O	-2.194039996	3.302255500	-1.228350186
C	3.609028960	0.204997960	0.381823560
C	3.120427324	-2.022504539	0.664444072
C	-3.587901924	-0.292543346	-0.966128540
C	3.275926678	-0.780426934	1.346023151
C	-3.470232494	-0.710922948	1.294153901
C	3.647658714	-0.420868753	-0.891247715
C	-3.267858016	-1.935227584	0.613051383
C	3.355478857	-1.799690612	-0.715231117
C	-3.338453976	-1.679020048	-0.786040828
C	1.364259303	2.422777311	-0.874386578
C	-3.661743751	0.303956724	0.318081001
C	-1.350526296	2.722951270	-0.719209429
B	0.078813576	-2.299328668	-0.062660036
C	0.303896250	2.973681393	1.402665845
B	-0.126482412	-1.473533315	1.450345535
B	-0.330925927	-1.491648195	-1.517364712
B	0.245906513	0.228393573	1.591234734
B	-0.127777148	0.331409951	-1.637120010
H	3.305123773	-2.542737328	-1.493841026
H	2.874118879	-2.966452202	1.119267932
H	3.873697247	0.066146173	-1.826251743

H	3.796230752	1.247358551	0.579305823
H	3.180895620	-0.623209633	2.406841541
H	-3.695235755	0.216284890	-1.910038202
H	-3.839542306	1.348117809	0.518463992
H	-3.468385200	-0.573346494	2.362920977
H	-3.087047845	-2.892092845	1.072589625
H	-3.243138199	-2.412369670	-1.568387892
H	-0.323496742	0.783252169	-2.721945859
H	-0.368886263	-2.026140548	-2.577230222
H	0.090839266	-3.489040115	-0.034062598
H	-0.068921441	-2.108999434	2.453841371
H	0.376105966	0.565854873	2.724020319
H	1.150168518	0.071476452	-1.797176676
H	-0.951413660	0.985008028	1.153343412

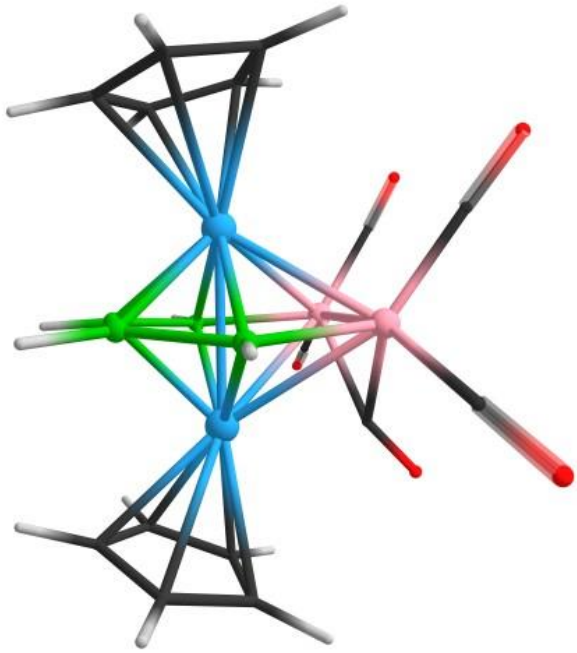

T.E = -3956.041390 a.u.

Highest imaginary frequency = -206.84 cm^{-1}

Figure S34. Optimized geometry of **II**

W	1.509861000	-0.467185000	-0.000012000
C	3.274414000	-2.064128000	-0.000182000
C	3.457020000	-1.250447000	1.151264000
C	3.732619000	0.066763000	0.711634000
W	-1.281573000	-0.815784000	-0.000048000
C	-3.583868000	-0.639146000	-0.708590000
C	-3.094674000	-1.899259000	-1.147144000
C	-2.807720000	-2.680517000	-0.000291000
Co	-0.216482000	1.273862000	-1.203854000

C	-1.791504000	2.078876000	-1.445689000
O	-2.789527000	2.577934000	-1.694212000
C	0.501736000	1.642695000	-2.800085000
O	0.955587000	1.874925000	-3.817583000
C	1.315037000	1.770629000	-0.000344000
O	2.053250000	2.687409000	0.000019000
B	0.217704000	-2.123821000	-0.862091000
H	0.421177000	-3.158779000	-1.411596000
B	0.155121000	-0.708218000	-1.814668000
H	0.161794000	-0.940296000	-2.982566000
C	3.456816000	-1.250447000	-1.151660000
C	3.732491000	0.066763000	-0.712081000
C	-3.583981000	-0.639209000	0.708003000
C	-3.094896000	-1.899371000	1.146564000
B	0.217543000	-2.123862000	0.862085000
H	0.420850000	-3.158835000	1.411631000
B	0.155697000	-0.708277000	1.814687000
H	0.162134000	-0.940413000	2.982574000
Co	-0.216411000	1.273780000	1.204121000
C	-1.791596000	2.078445000	1.446350000
O	-2.789693000	2.577213000	1.695105000
C	0.501822000	1.641900000	2.800490000
O	0.955928000	1.873796000	3.817948000
H	-2.415829000	-3.683190000	-0.000299000
H	-2.970135000	-2.210801000	-2.170837000
H	-3.914963000	0.166554000	-1.342213000
H	-3.915181000	0.166447000	1.341631000
H	-2.970547000	-2.210996000	2.170255000
H	3.911379000	0.924791000	1.338978000
H	3.391490000	-1.579534000	2.174725000
H	3.053414000	-3.117470000	-0.000163000
H	3.391094000	-1.579533000	-2.175109000
H	3.911159000	0.924781000	-1.339463000

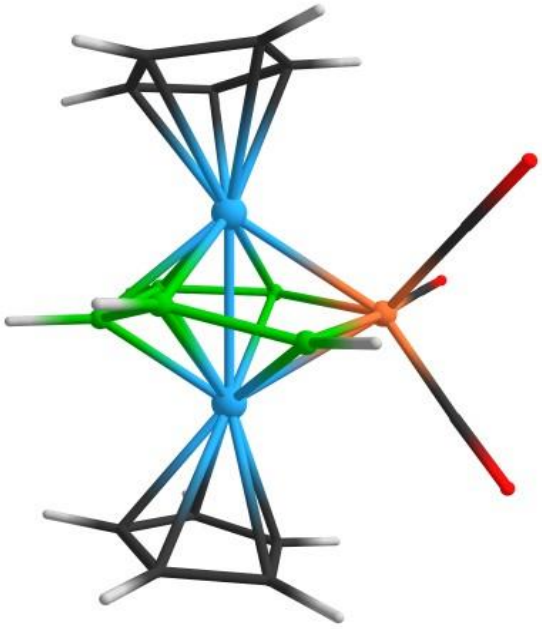

T.E =-2252.807275a.u.

Figure S35. Optimized geometry of **III**

W	8.900166000	3.213257000	13.433985000
W	6.922680000	3.455355000	15.359761000
Fe	6.972565000	5.097386000	13.358519000
O	6.958539000	4.781853000	10.422624000
O	7.841044000	7.898104000	13.235569000
O	4.117476000	5.678784000	13.783132000
C	10.260191000	3.834955000	11.544738000
C	11.112702000	2.352908000	13.072399000
C	4.635855000	3.286055000	16.137747000
C	11.131647000	3.709344000	12.653275000
C	6.273799000	4.017893000	17.573661000
C	9.699427000	2.555188000	11.279497000
C	6.330063000	2.600037000	17.533406000
C	10.234033000	1.635027000	12.217587000
C	5.326345000	2.153676000	16.639285000
C	6.968104000	4.904119000	11.560010000
C	5.217866000	4.441990000	16.715794000
C	5.226010000	5.435092000	13.639896000
B	8.534988000	2.018491000	15.392599000
C	7.511850000	6.806029000	13.280820000
B	9.325977000	3.564482000	15.459164000
B	7.562436000	1.641799000	14.045586000
B	8.587981000	5.043538000	14.628407000
B	6.429097000	2.833259000	13.403959000
H	10.009718000	0.583608000	12.273856000
H	11.670511000	1.939828000	13.895704000

H	8.989141000	2.324140000	10.501288000
H	10.055457000	4.740764000	10.997819000
H	11.702446000	4.502683000	13.106525000
H	3.811467000	3.268809000	15.444769000
H	4.904255000	5.459452000	16.553444000
H	6.911857000	4.659467000	18.160433000
H	7.022087000	1.976590000	18.073122000
H	5.133614000	1.128082000	16.371045000
H	5.692178000	2.496804000	12.537398000
H	7.274415000	0.513300000	13.801661000
H	9.012883000	1.138305000	16.035611000
H	10.086931000	3.854142000	16.322397000
H	9.087184000	5.996566000	15.135436000

III Supplementary Data

Table S5 Examples of electron poor triple-decker sandwich complexes and their valence electron count (VEC).

Sl no.	Compound	VEC	d(M-M)
1.	$[(Cp^*Re)_2\{\mu\text{-}\eta^6\text{:}\eta^6\text{-}B_4H_4Co_2(CO)_5\}]$[18]	24	2.6393(5)
2.	$[(Cp^*Re)_2\{\mu\text{-}\eta^6\text{:}\eta^6\text{-}B_4H_4Cl_2]$[19]	24	2.6887(5)
3.	$[(Cp^*Mo)_2\{\mu\text{-}\eta^6\text{:}\eta^6\text{-}B_3H_3TeCo_2(CO)_5\}]$[20]	24	2.7520(6)
4.	$[(Cp^*Mo)_2\{\mu\text{-}\eta^6\text{:}\eta^6\text{-}B_4H_4Ru_2(CO)_6\}]$[21]	22	2.7510(5)
5.	$[(Cp^*Mo)_2\{\mu\text{-}\eta^6\text{:}\eta^6\text{-}B_4H_4SRu(CO)_3\}]$[22]	24	2.7693(3)
6.	$[(Cp^*Mo)_2\{\mu\text{-}\eta^6\text{:}\eta^6\text{-}B_4H_4SeRu(CO)_3\}]$[22]	24	2.7733(7)
7.	$[(Cp^*Mo)_2\{\mu\text{-}\eta^6\text{:}\eta^6\text{-}B_4H_4TeRu(CO)_3\}]$[22]	24	2.7787(6)
8.	$[(Cp^*Co)_2\{\mu\text{-}B_2H_2S_2Pd(Cl)_2\}]$[23]	--[a]	3.207
9.	$[(Cp^*Co)_2\{\mu\text{-}B_2H_2Se_2Pd(Cl)_2\}]$[23]	--[a]	3.220
10.	$[(Cp^*Rh)_2\{\mu\text{-}B_2H_2Se_2Pd(Cl)_2\}]$[23]	--[a]	3.519
11.	$[(Cp^*Ir)_2\{\mu\text{-}B_2H_2ESe_2Pd(Cl)_2\}]$[23]	--[a]	--
12.	**1**	24	2.7510(5)
13.	**4**	24	2.769(2)

[a]Although the entries 8-11 in Table S1 are triple-decker structures, they are considerebly different from others metallaboane/heteroborane triple-decker clusters. They have been generated by the coordination of $PdCl_2$ fragment to the open-cage triple-decker. Hence, the exact electron

contribution from the middle-deck towards the cluster is not clear to us yet. This needs further studies and understanding, thus, we are not able to provide the data.

References;

1) (a) Dhayal, R. S.; Sahoo, S.; Ramkumar, V.; Ghosh, S. Substitution at boron in molybdaborane frameworks: Synthesis and characterization of isomeric $(\eta^5\text{-}C_5Me_5Mo)_2B_5H_nX_m$ (when X=Cl: *n*=5, 7, 8; *m*=4, 2, 1 and X=Me: *n*=6, 7; *m*=3, 2). *J. Organomet. Chem.* **2009**, *694*, 237−243. (b) Green, M. L. H.; Hubert, J. D.; Mountford, P. Synthesis of the W≡W triply bonded dimers $[W_2(\eta^5\text{-}C_5H_4R)_2X_4]$(X = Cl, R = Me or Pri; X = Br, R = Pri) and X-ray crystal structures of $[W(\eta^5\text{-}C_5H_4Pri)Cl_4]$ and $[W_2(\eta\text{-}C_5H_4Pri)_2Cl_4]$. *J. Chem. Soc. Dalton Trans.* **1990**, 3793−3800. (c) Kaushika, M.; Singh, A.; Kumar, M. The chemistry of group-VIb metal carbonyls. *Eur. J. Chem.* **2012**, *3*, 367−394.
2) Ryschkewitsch, G. E.; Nainan, K. C. Octahydrotriborate(1-) $[B_3H_8]$ salt. *Inorg. Synth*. **1974**, *15*, 113−114.
3) Weller, A. S.; Shang, M.; Fehlner, T. P. Synthesis of Mono- and Ditungstaboranes from Reaction of Cp^*WCl_4 and $[Cp^*WCl_2]_2$ with BH_3·thf or $LiBH_4$ ($Cp^* = \eta^5\text{-}C_5Me_5$). Control of Reaction Pathway by Choice of Monoboron Reagent and Oxidation State of Metal Center. *Organometallics* **1999**, *18*, 53-64.
4) Bag, R.; Kar, S.; Saha, S.; Gomosta, S.; Raghavendra, B.; Roisnel, T.; Ghosh, S. Heterometallic Triply-Bridging Bis-Borylene Complexes. *Chem. Asian. J*. **2020**, *15*, 780 –786.
5) Sheldrick, G. M. *Acta Cryst*. **2015**, *A71*, 3-8
6) Sheldrick G.M., *Acta Cryst*. **2015**, *C71*, 3-8
7) Dolomanov, O.V.; Bourhis, L.J.; Gildea, R.J.; Howard, J.A.K.; Puschmann, H., OLEX2: A complete structure solution, refinement and analysis program. J. Appl. Cryst. **2009**, *42*, 339-341.
8) Gaussian 16, Revision C.01, Frisch, M. J.; Trucks, G. W.; Schlegel, H. B.; Scuseria, G. E.; Robb, M. A.; Cheeseman, J. R.; Scalmani, G.; Barone, V.; Petersson, G. A.; Nakatsuji, H.; Li, X.; Caricato, M.; Marenich, A. V.; Bloino, J.; Janesko, B. G.; Gomperts, R.; Mennucci, B.; Hratchian, H. P.; Ortiz, J. V.; Izmaylov, A. F.; Sonnenberg, J. L.; Williams-Young, D.; Ding, F.; Lipparini, F.; Egidi, F.; Goings, J.; Peng, B.; Petrone, A.; Henderson, T.; Ranasinghe, D.; Zakrzewski, V. G.; Gao, J.; Rega, N.; Zheng, G.; Liang, W.; Hada, M.; Ehara, M.; Toyota, K.; Fukuda, R.; Hasegawa, J.; Ishida, M.; Nakajima, T.; Honda, Y.; Kitao, O.; Nakai, H.; Vreven, T.; Throssell, K.; Montgomery, J. A., Jr.; Peralta, J. E.; Ogliaro, F.; Bearpark, M. J.; Heyd, J. J.; Brothers, E. N.; Kudin, K. N.; Staroverov, V. N.; Keith, T. A.; Kobayashi, R.; Normand, J.; Raghavachari, K.; Rendell, A. P.; Burant, J. C.; Iyengar, S. S.; Tomasi, J.; Cossi, M.; Millam, J. M.; Klene, M.; Adamo, C.; Cammi, R.; Ochterski, J. W.; Martin, R. L.; Morokuma, K.; Farkas, O.; Foresman, J. B.; Fox, D. J. Gaussian, Inc., Wallingford CT, 2016.

9) Lee, C.; Yang, W.; Parr. R. G. Development of the Colle-Salvetti correlation-energy formula into a functional of the electron density. *Phys. Rev. B*. **1988**, *37*, 785-789.

10) a) Schmider, H. L.; Becke, A. D. Optimized density functionals from the extended G2 test set. *J. Chem. Phys*. **1998**, *108*, 9624-9631. b) Perdew, J. P. Density-functional approximation for the correlation energy of the inhomogeneous electron gas. *Phys.Rev. B* **1986**, *33*, 8822-8824.

11) a) Weigend, F.; Ahlrichs, R. Balanced basis sets of split valence, triple zeta valence and quadruple zeta valence quality for H to Rn: Design and assessment of accuracy. *Phys. Chem. Chem. Phys.* **2005**, *7*, 3297–3305. b) Weigend, F. Accurate Coulomb-fitting basis sets for H to Rn. *Phys. Chem. Chem. Phys.* **2006**, *8*, 1057-1065.

12) Andrae, D.; Häußermann, U.; Dolg, M.; Stoll, H.; Preuß, H. Energy-adjusted ab initio pseudopotentials for the second and third row transition elements. *Theor. Chim. Acta.* **1990**, *77*, 123-141.

13) a) London, F. J., Théorie quantique des courants interatomiques dans les combinaisons aromatiques. *J. Phys. Radium* **1937**, *8*, 397–409. b) Ditchfield, R. Self-consistent perturbation theory of diamagnetism. *Mol. Phys.* **1974**, *27*, 789–807. c) Wolinski, K.; Hinton J. F.; Pulay, P. Efficient Implementation of the Gauge-Independent Atomic Orbital Method for NMR Chemical Shift Calculations. *J. Am. Chem. Soc.* **1990**, *112*, 8251–8260.

14) Onak, T. P.; Landesman, H. L.; Williams, R. E.; Shapiro, I. The B11 Nuclear Magnetic Resonance Chemical Shifts and Spin Coupling Values for Various Compounds. *J. Phys. Chem.* **1959**, *63*, 1533–1535.

15) Wiberg, K., Application of the Pople-Santry-Segal CNDO method to the cyclopropylcarbinyl and cyclobutylcation and to bicyclobutane. *Tetrahedron* **1968**, *24*, 1083–1096.

16) a) Reed, A. E.; Curtiss, L. A.; Weinhold, F. Intermolecular Interactions from a Natural Bond Orbital, Donor-Acceptor Viewpoint. *Chem. Rev.* **1988**, *88*, 899–926. b) Weinhold, F.; Landis, C. R. Valency and Bonding: A Natural Bond Orbital Donor-Acceptor Perspective; Cambridge University Press, Cambridge, **2005**. c) King, R. B. Topological Aspects of the Skeletal Bonding in “Isocloso” Metallaboranes Containing “Anomalous” Numbers of Skeletal Electrons. *Inorg. Chem.* **1999**, *38*, 5151–5153. d) King, R. B. Face-Localized Bonding Models for Borane Cage Ligands in Transition Metal Coordination Chemistry. *Inorg. Chim. Acta.* **2000**, *300*, 537–544.

17) Chemcraft - graphical software for visualization of quantum chemistry computations. https://www.chemcraftprog.com

18) Ghosh, S.; Shang, M.; Fehlner, T. P. A Novel Coordinated Inorganic Benzene: Synthesis and Characterization of $\{\eta^5\text{-}C_5Me_5Re\}_2\{\mu\text{-}\eta^6\text{:}\eta^6\text{-}B_4H_4Co_2(CO)_5\}$. *J. Am. Chem. Soc*. **1999**, *121*, 7451−7452.

19) Ghosh, S.; Beatty, A. M.; Fehlner, T. P. Synthesis and Characterization of Bicapped Hexagonal Bipyramidal 2,3-Cl_2-1,8-$\{Cp^*Re\}_2B_6H_4$[$\{Cp^*Re\}_2\{\mu\text{-}\eta^6\text{:}\eta^6\text{-}1,2\text{-}B_6H_4Cl_2\}$, $Cp^* = \eta^5\text{-}C_5Me_5$]: The Missing Link Connecting (p−2) Skeletal Electron Pair Hypoelectronic Rhenaboranes and 24-Valence Electron Triple-Decker Complexes. *J. Am. Chem. Soc.* **2001**, *123*, 9188-9189.

20) Thakur, A.; Chakrahari, K. K. V.; Mondal, B.; Ghosh, S. Novel Triple Decker Sandwich Complex with a Six-Membered [$B_3Co_3(\mu^4$-Te)] Ring as the Middle Deck. *Inorg. Chem*. **2013**, *52*, 2262−2264.

21) Mondal, B.; Mondal, B.; Pal, K.; Varghese, B.; Ghosh, S. An electron-poor di-molybdenum triple-decker with a puckered [B_4Ru_2] bridging ring is an oblato-closo cluster. *Chem. Commun.* **2015**, *51*, 3828-3831.

22) Mondal, B.; Bhattacharyya, M.; Varghese, B.; Ghosh, S. Hypo-electronic triple-decker sandwich complexes: synthesis and structural characterization of [$(Cp^*Mo)_2\{\mu$–η^6:η^6-B_4H_4E-$Ru(CO)_3\}$] (E = S, Se, Te or $Ru(CO)_3$ and Cp* = η^5-C_5Me_5). *Dalton Trans.* **2016**, *45*, 10999-11007.

23) Joseph, B.; Prakash, R.; Bag, R.; Ghosh, S. “Triple-Decker Sandwich” Containing Planar {B_2E_2Pd} Ring (E = S or Se). *Inorg. Chem.* **2020**, *59*, 16272–16280.